

## BIODESULFURIZATION OF FLUE GASES USING SYNTHESIS GAS DELIVERED AS MICROBUBBLES

Punjai T. Selvaraj\*, Marshall D. Bredwell,  
Mark H. Little, and Eric N. Kaufman  
Bioprocessing Research and Development Center  
Oak Ridge National Laboratory  
Bldg. 4505, MS 6226  
Oak Ridge, Tennessee 37831-6226

Keywords: Biodesulfurization, synthesis gas, microbubbles

### Introduction

Anaerobic treatment processes for biodegradation of hazardous materials have increasingly been gaining attention in environmental applications. Microbial processes utilizing sulfate reducing bacteria (SRB), in particular, have found potential applications in variety of treatment processes such as flue gas desulfurization [1,2], gypsum reclamation [3], sulfur recovery from sulfite/sulfate wastewater from pulp and paper, chemical and mining industries [4], and degrading explosive materials [5]. However, in all these applications, the source of electron donor is a major factor on the economics of the process. Previously, we have proposed a microbial process with sewage digest as an attractive low-cost feedstock for SRB cultures in the desulfurization of flue gases and sulfite/sulfate-laden industrial waste water [6]. In that process, a columnar reactor with mixed SRB cultures immobilized in BIO-SEP™ polymeric porous beads with sewage digest as a carbon and energy source exhibited conversion rate of 16.5 mmol sulfite/h•L (32 kg/d•m<sup>3</sup>) with 100% conversion to H<sub>2</sub>S. Though municipal sewage digest is a readily available low-cost carbon source, the real cost of the medium depends on the location of the sewage treatment plant and power plant and on the transportation involved in bringing the sewage back and forth from the sewage plant. Therefore, the current research has been focused on an alternative low-cost feedstock. Various groups have demonstrated that SRB could be supported by carbon dioxide and/or carbon monoxide as the sole carbon source and hydrogen as the energy source [7-11]. Du Preez et al. [8,10] operated a sulfate-reducing reactor with a mixed SRB population to demonstrate the feasibility of using syn-gas as the feed source for SRB. Recently, van Houten et al. [9] reported the operation of a gas-lift sulfate-reducing reactor that was fed a CO-H<sub>2</sub> mixture (up to 20% CO) and yielded a maximum sulfate conversion rate of 30 g SO<sub>4</sub><sup>2-</sup>/d•L.

In our study, we have focused our research on utilizing gas mixture containing 36% H<sub>2</sub>, 47% CO, 10% CO<sub>2</sub>, 5% CH<sub>4</sub> and balance N<sub>2</sub> as a model coal synthesis gas as a low-cost feedstock. This composition is typical of an oxygen blown, coal fed gasifier. Coal synthesis gas will be readily available in power plants and the biological utilization of syn-gas as a carbon and energy source produces no organic end product that has to be processed prior to its disposal. Coal synthesis gas is, however, sparingly soluble in aqueous phase. Our process utilizing SRB with syn-gas feedstock may be mass transfer limited and methods to enhance the mass transport have been investigated. A CSTR with cell recycle and a trickle bed reactor with cells immobilized in BIO-SEP™ polymeric beads were operated with syn-gas feedstock to obtain maximum productivity for SO<sub>2</sub> reduction to H<sub>2</sub>S. The CSTR reactor was then fed with syn-gas as microbubbles in an effort to improve the mass transfer properties.

### Materials and Methods

#### Microbial Culture and Media

Mixed SRB cultures were originally isolated from sewage solids obtained from the DAF unit of a municipal sewage treatment plant at Oak Ridge, TN. The cultures were grown in lactic acid media (LA) which consists of 3.6 g/L citric acid, 0.8 g/L CaCl<sub>2</sub>, 1.0 g/L NH<sub>4</sub>Cl, 0.5 g/L K<sub>2</sub>HPO<sub>4</sub>, 1.0 g/L yeast extract, 0.52 g/L FeCl<sub>2</sub>, 5.8 mL/L of sodium lactate (60% syrup), 0.518 mL/L butyric acid, and 0.05 g/L cysteine HCL. A minimal salts media (MS) was also used; 1.2 g/L Na<sub>2</sub>HPO<sub>4</sub>, 1.8 g/L KH<sub>2</sub>PO<sub>4</sub>, 0.7 g/L MgCl<sub>2</sub>, 0.2 g/L NH<sub>4</sub>Cl, 0.04 g/L FeCl<sub>3</sub>, 50 mL/L mineral water, 0.2 mL/L Batch vitamin solution, and 15 mL/L heavy metal solution (HMS). The Batch vitamin solution contains the following: 2.0 mg/L biotin, 2.0 mg/L folic acid, 10.0 mg/L pyridoxine hydrochloride, 5.0 mg/L thiamine

hydrochloride, 5.0 mg/L riboflavin, 5.0 mg/L nicotinic acid, 5.0 mg/L DL-calcium pantothenate, 0.1 mg/L vitamin B-12, 5.0 mg/L p-amino benzoic acid, and 5.0 mg/L lipoic acid. The HMS solution contains the following: 1.5 g/L EDTA, 0.1 g/L  $ZnSO_4 \cdot 7H_2O$  and 6 mL/L of a trace element solution (0.0507 g/L  $AlCl_3$ , 0.139 g/L KI, 0.139 g/L KBr, 0.139 g/L LiCl, 3.060 g/L  $H_3BO_3$ , 0.280 g/L  $ZnCl_2$ , 0.326 g/L  $CuCl_2 \cdot 2H_2O$ , 0.513 g/L  $NiCl_2 \cdot 6H_2O$ , 0.513 g/L  $CoCl_2 \cdot 6H_2O$ , 0.139 g/L  $SnCl_2 \cdot 2H_2O$ , 0.163 g/L  $BaCl_2 \cdot 2H_2O$ , 0.139 g/L  $Na_2MoO_4 \cdot 2H_2O$ , 0.139 g/L  $CuSeO_4 \cdot 5H_2O$ , and 0.024 g/L  $NaVO_3$ ).

In serum bottles, the sulfate source was provided by the addition of up to 4.0 g/L of  $Na_2SO_4$  or  $MgSO_4$ . In the reactors, the sulfite source was provided by a gas mixture containing 5%  $SO_2$ , 5%  $CO_2$ , and balance  $N_2$ . For growth on synthesis gas, a mixture of 47%  $CO$ , 36%  $H_2$ , 10%  $CO_2$ , 5%  $CH_4$ , and the balance  $N_2$  was used. For serum bottle studies, 100 mL of MS media was put into a ~150 mL bottle and sealed with butyl rubber stopper. A nitrogen headspace was placed on top of the media and the bottles were sterilized by steam. When inoculated from an actively growing culture in a 2 L chemostat, synthesis gas was bubbled through the culture. The headspace was monitored for synthesis gas components and hydrogen sulfide and was replenished with fresh synthesis gas when needed. The bottles were usually shaken at 100 rpm at 30°C.

#### *Syn-Gas Utilization by Mixed SRB*

Utilization of syn-gas by mixed SRB culture developed from municipal sewage was investigated in a serum bottle containing minimal salt medium and  $SO_2$  as terminal electron acceptor. The head space of the bottle was then filled with synthesis gas mixture containing 36%  $H_2$ , 47%  $CO$ , 10%  $CO_2$ , 5%  $CH_4$ , and balance  $N_2$ . The bottle was inoculated with mixed SRB culture and incubated at 30°C with shaking at 200 rpm. The syn-gas concentration was then regularly monitored using a Gas Chromatograph as described below.

#### *Microbubble Generation and Characterization*

Microbubbles are small, surfactant coated bubbles of gas that are generated by creating a gas-liquid interface in a high-shear zone. The bubbles are between 50  $\mu m$  and 100  $\mu m$  in diameter and the surfactant coating helps to prevent coalescence by electrostatic repulsion from the diffuse electric double layer around the bubble. In our work, the microbubble dispersions were generated using a spinning disk apparatus first described by Sebba [12]. This microbubble generator (MBG) uses a high speed motor (Talboys #37830, Cole Parmer, Chicago, IL) that spins a 4 cm disk as speeds above 4000 RPM in close proximity to baffles (within 3 mm) to generate a localized high-shear zone. The stainless steel disk and baffles are mounted in 4 L glass vessel with a ground glass lip to fit the headplate. A second headplate mounted above the first supports the motor and allows easy alignment. Stainless steel sealed bearings insure minimal wobble.

The bubble size measurements were performed on a Coulter LS 130 particle size analyzer (Coulter) using laser diffraction. The microbubble foam sample was loaded into both the constant volume module and hazardous fluids module for the instrument. The constant volume module could contain 15 mL of sample and had a magnetic stirrer in the bottom of the cell to maintain a well-mixed system. The hazardous fluids module used a recirculating pump. Dispersion was added to water in each module until 8% to 12% obscuration was obtained. Data was collected for ninety seconds in each case. Between runs the constant volume module was rinsed with double distilled water and the hazardous fluids modules had the recirculating liquid drained, refilled, and filtered.

#### *CSTR and Trickle Bed Reactors*

A 2 L Virtis Omni-culture chemostat (Virtis Co., Gardiner, NY) with temperature and agitation control was used as the primary reactor vessel. The vessel headplate was modified for acid/base additions and gas and liquid inlets and outlets. The pH was controlled at 6.8 with a Chemcadet controller with 6 N NaOH and 6 N  $H_3PO_4$ . The reactor was maintained at a temperature of 30°C and agitated at 250 rpm for all experimental runs. The reactor was operated in a continuous mode with a feed rate of fresh MS medium at 0.2 mL/min. To retain biomass in the reactor, a filtration system consisted of two Amicon Diaflo hollow fiber cartridges was attached to the reactor. All pumps used were Masterflex peristaltic. A sparge of 50 mL/min of nitrogen was added to the reactor vessel to strip off the produced  $H_2S$  from the reactor. The synthesis gas was fed directly at a rate

of 10 mL/min to the reactor during the control runs through a stainless steel sparger. The flow rate of SO<sub>2</sub> gas fed separately into the reactor was monitored using gas flow meter. In the microbubble-fed system, the permeate from the filters was returned to the MBG, the syn-gas microbubbles were generated by bubbling syn-gas into minimal salt medium containing Tween-20 (240 mg/L) as surfactant. The microbubbles were then fed to the CSTR at a rate of 15 mL/min, which was equivalent to 10 mL/min of synthesis gas as fed during the control run.

The trickle bed reactor consisted of fully jacketed glass column of internal dimensions 2.5 x 30 cm with a total volume of 180 mL and a working volume of 81 mL with BIO-SEP™ beads. BIO-SEP™ beads, encapsulated activated carbon (50-80%) in aromatic polyamide (Aramid) (20-50%) were obtained as the kind gift of Dr. Carl Camp from the DuPont Chemical Co. (Glasgow, DE). The reactor was operated at a temperature of 30°C. A 500 mL bottle with a specially made headplate was used for pH control, H<sub>2</sub>S stripping by nitrogen, gas outlet, and ports for continuous operation. The reactor had biomass loaded on to the BIO-SEP beads by operation in a packed bed mode on lactate media. The liquid inside of the reactor was completely recycled. When switched to a synthesis gas feed, the reactor was operated in a trickle bed mode with the liquid and both gas feeds entering at the top of the reactor. Gas samples were taken from a gas disengagement bottle. The reactor was operated in a continuous mode with a fresh minimal salt medium at a feed rate of 12 mL/h. In trickle bed mode, the liquid flow rate across the bed was 600 mL/h.

In all runs the reactor was monitored for sulfite. The off-gas from the reactor was also monitored for H<sub>2</sub>S and synthesis gas components. The off-gas flow rates were monitored with a wet test meter for two hour periods.

#### Analytical

The sulfite in the reactor was analyzed spectrophotometrically by the reaction of fuchsin and formaldehyde in sulfuric acid [13]. The sulfide in the reactor was precipitated using zinc acetate in a basic solution followed by resuspension and measurement using the formation of methylene blue [14].

Hydrogen sulfide in the off gas was analyzed using a gas chromatograph (Hewlett Packard HP 5890 Series II) equipped with a teflon column (30 in x 1/8 in) packed with Super Q (80/100 mesh) (Alltech, Waukegan, WI). Temperatures of the column, injection port, and thermal conductivity detector were 70°C, 125°C, and 125°C respectively. The carrier gas was helium at 25 mL/min. The calibration was based on 1%, 5%, and 10% H<sub>2</sub>S in nitrogen standards. Synthesis gas components were measured using a gas chromatograph (Hewlett Packard HP 5890 Series II) equipped with a HP PLOT molecular sieve 5 Å capillary column (30 m x 0.32 mm) with a 12 µm film thickness. Temperatures on the column, injection port, and thermal conductivity detector were 55°C, 100°C, and 240°C respectively. Liquid samples were filtered through a 0.22 µm syringe filter and analyzed by gas chromatography using a HP 5890 Series II with a HP WAT (crosslinked PEG) capillary column (30 m x 0.53 mm) with a 1.0 µm film thickness. The column temperature program was initially 70°C followed by ramping to 200°C at 25°C/min with a 1.2 min hold then followed by ramping to 225°C at 25°C/min with a 3.0 min hold. The injection port temperature was 245°C while the flame ionization detector was 265°C.

## Results and Discussion

### *Syn-Gas Utilization by Mixed SRB*

Initially, a decrease in CO concentration was observed with no change in H<sub>2</sub> concentration. However, hydrogen sulfide was detected during this time in the head space of the serum bottle. This indicates that the CO was utilized by certain type of bacteria and produced H<sub>2</sub> as shown in the equation below:



With limited SO<sub>2</sub> reduction due to a possible CO inhibition at higher concentration, the H<sub>2</sub> concentration declined only after the CO concentration was less than about 5% in the mixture. This suggests that the mixed culture developed from sewage solids would be

able to use CO as sole carbon and energy source and produce H<sub>2</sub>. Kinetically, the CO utilization was much faster than H<sub>2</sub> utilization by SRB cultures.

Serum bottle experiments with mixed SRB showed that we could switch between lactate and syn-gas for carbon and energy source that would help us to start the reactor operation more quickly.

#### *CSTR with syn-gas feed*

The CSTR in the control mode in which the syn-gas was fed directly into the reactor was able to convert 1.2 mmol SO<sub>2</sub>/h•L with no sulfite detected in the effluent (Fig. 1). The off-gas analysis through GC showed 100% conversion of SO<sub>2</sub> into H<sub>2</sub>S. With continuous N<sub>2</sub> purging in the liquid medium, the sulfide concentration in the aqueous phase was measured to be less than 5 mg/L. When the SO<sub>2</sub> feed was increased above 1.2 mmol/h•L, sulfite accumulation of greater than 25 mg/L was observed in the reactor medium. This indicated that the reactor reached the maximum productivity of 1.2 mmol SO<sub>2</sub>/h•L under the operating conditions. The synthesis gas content in the feed and the off-gas showed the stoichiometric conversion of 1.8 mol H<sub>2</sub> and 2.3 mol CO per mol of SO<sub>2</sub>. The reactor was then operated at 1.2 mmol/h•L, for 3 d and switched over to microbubble-fed system. With syn-gas fed as microbubbles, the SO<sub>2</sub> feed rate was increased incrementally and the maximum productivity of 2.1 mmol/h•L was obtained with 100% conversion to H<sub>2</sub>S in 33 h. The biomass concentration in the reactor prior to the microbubble operation was 5 g/L. The increase of productivity from 1.2 to 2.1 mmol/h•L within the span of 33 h at the same biomass concentration of 5 g/L indicated that the mass transport of syn-gas was the limiting parameter in the above process.

#### *Trickle-bed reactor with syn-gas feed*

Initially, the immobilization of mixed SRB cells in BIO-SEP beads in a trickle-bed reactor was started-up with lactate medium as described earlier. This was achieved in 14 d. Following the immobilization, the reactor was fed with syn-gas at a rate of 10 mL/min as a sole carbon and energy source and 5% SO<sub>2</sub> at rate of 4 mL/min (2.7 mmol/h•L). The immobilized SRB cells grown on lactate medium were able to switch to syn-gas at once. The SO<sub>2</sub> feed rate was then increased incrementally with no sulfite detected in the effluent. As shown in Fig. 2, complete conversion of SO<sub>2</sub> into H<sub>2</sub>S was achieved at a maximum SO<sub>2</sub> feed of 8.8 mmol/h•L with syn-gas utilization of 1.0 mol H<sub>2</sub> and 1.2 mol CO per mol of SO<sub>2</sub>. This compares to previous studies which achieved 4.3 mmol SO<sub>4</sub><sup>2-</sup>/h•L [9] and 0.5 mmol/h•L [10] with synthesis gas as feedstock.

#### **Conclusion**

The model coal synthesis gas containing 36% H<sub>2</sub>, 47% CO, 10% CO<sub>2</sub>, 5% CH<sub>4</sub>, and balance N<sub>2</sub> has been found as a low-cost feedstock for mixed SRB in the desulfurization processes. With syn-gas fed as microbubbles, productivity in the CSTR increased from 1.2 to 2.1 mmol/h•L in 33 h. This has been observed at the same biomass concentration of 5 g/L. This shows the mass transport limitation in the above process. In the trickle bed reactor, maximum productivity of 8.8 mmol/h•L was achieved with less carbon and energy requirement (1 mol H<sub>2</sub> and 1.2 mol CO per mol of SO<sub>2</sub>) indicating better surface to volume ratio with cells immobilized in the pores of polymeric beads. The mass transfer coefficients in these systems will be determined in future studies to develop better reactor configuration for biodesulfurization of flue gases and other sulfur wastes.

#### **References**

1. Selvaraj, P.T., and Sublette, K.L. (1995), *Biotechnol. Prog.* **11**, 153-158.1.
2. Paques B.V. and Hoogovens Technical Services (1995), *Bio-technological Flue Gas Desulfurization Report*.
3. Kaufman, E.N., Little, M.H., and Selvaraj, P.T. (1996), *J. Chem. Technol. Biotechnol.* **66**, 365-374.
4. Hammack, R.W., Edenborn, H.M., and Dvorak, D.H. (1994), *Water Res.* **28**, 11, 2321-2329.
5. Boopathy, R., and Manning, J.F. (1996), *American Academy of Environmental Engineers*, Washington DC. pp 61-75.
6. Selvaraj, P.T., Little, M.H., and Kaufman, E.N. (1996), submitted to *Bioremediation*.

7. van Houten, R.T., Pol, L.W.H., and Lettinga, G. (1994), *Biotechnol. Bioeng.* **44**, 586-594.
8. Du Preez, L.A., Odendaal, J.P., Maree, J.P., and Posonby, M. (1992), *Environ. Technol.* **13**, 875-882.
9. van Houten R.T., van der Spoel, H., van Aelst, A.C., Hulshoff Pol, L.W., and Lettinga, G. (1996), *Biotechnol. Bioeng.* **50**, 136-144.
10. Du Preez, and Maree, J.P., (1992), *Water Sci. Tech.* **30**, 275-285.
11. Kaufman, E.N., Little, M.H., and Selvaraj, P.T. (1996), *Appl. Biochem. Biotechnol.* (in press).
12. Sebba, F. (1985), *Chemistry and Industry*, 91-92.
13. Steigman, A. (1950), *Anal. Chem.* **22**, 492-493.
14. Tanner, R. S. (1989), *J. Microbiological Methods*.

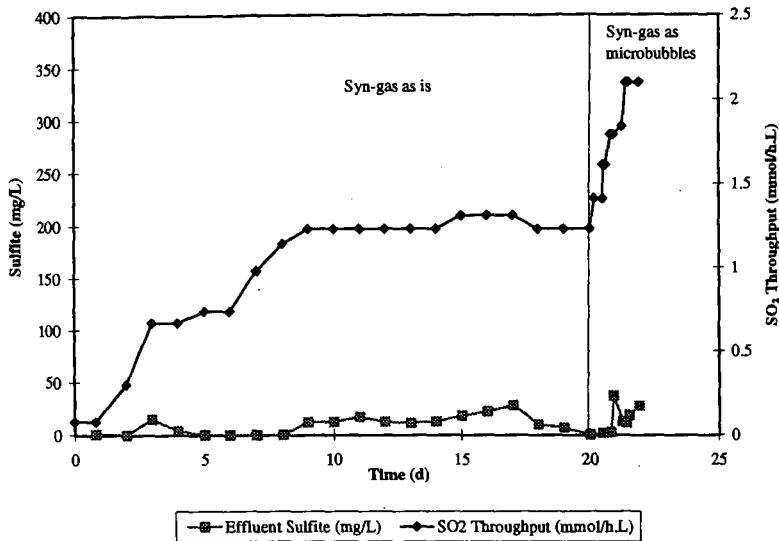


Figure 1. Sulfite conversion in a CSTR with syn-gas as feedstock. With syn-gas fed as microbubbles, the reactor productivity was increased from 1.2 to 2.1 mmol/h.L in 33 h.

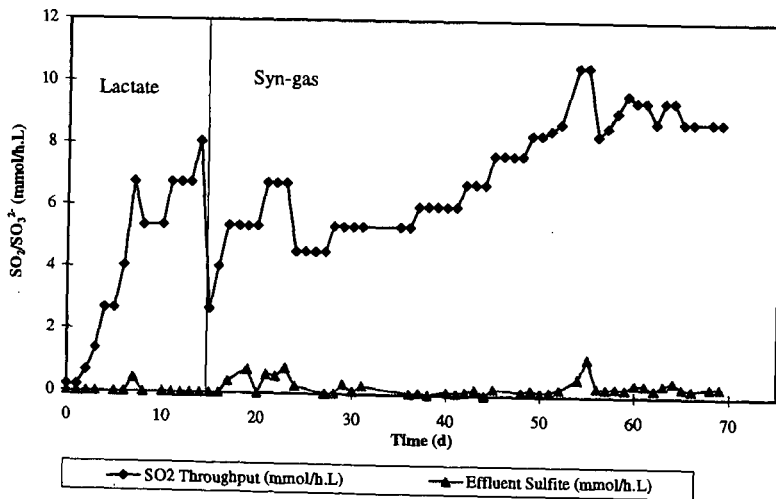


Figure 2. Sulfite conversion in a trickle-bed reactor with mixed SRB immobilized in BIO-SEP™ beads. The liquid medium and gas mixture (syn-gas and SO<sub>2</sub>) were fed co-currently at the top of the reactor.

# MICROBIAL DESULFURIZATION OF DIBENZOTHIOPHENE AND ITS DERIVATIVES

Yoshikazu Izumi and Takashi Ohshiro  
Department of Biotechnology, Faculty of Engineering,  
Tottori University, Tottori, 680 JAPAN

Keywords: desulfurization, dibenzothiophene, Rhodococcus

## INTRODUCTION

The serious environmental problem of acid rain is at least partly caused by the combustion of sulfur compounds present in the fossil fuels, releasing sulfur dioxide into the atmosphere. Though inorganic sulfur can be reduced by physical or chemical means, none of them can be applied to removing organic sulfur from petroleum. Therefore, microbial processes that can do so have recently received much focus. Dibenzothiophene (DBT) and its derivatives have been widely used as model organic sulfur compounds in petroleum (1). Three pathways of DBT degradation have been reported. The first is the ring-destructive pathway, in which the sulfur of DBT remains (2-5), the second is the completely destructive pathway, in which DBT is mineralized to carbon dioxide, sulfite and water (6), and the third is the sulfur-specific pathway, in which only sulfur is removed from DBT (7-9) as illustrated in Fig. 1. Strains having the second or third pathways should be applied to the microbial desulfurization process. In other studies, we also isolated a DBT-degrading bacterium, *Rhodococcus erythropolis* D-1, which has the sulfur-specific pathway (10) and observed an enzyme system catalyzing this conversion (11). Many research groups have since studied the desulfurization of DBT by the sulfur-specific pathway (12-14). The genes involved in DBT degradation have been identified (15-17). However, there has so far been little report on the DBT desulfurization in the presence of hydrocarbon. Since petroleum should ideally be desulfurized, we isolated a strain with the capacity to desulfurize DBT in the presence of hydrocarbon. Here we describe the desulfurization of DBT by growing whole cells of *Rhodococcus erythropolis* H-2 in the presence of n-tetradecane (TD) and other hydrocarbons. We also describe the desulfurization of substituted DBTs which actually exist in petroleum by *R. erythropolis* H-2 in the presence of TD.

## MATERIALS AND METHODS

Medium A-1 was the same as medium A described elsewhere (10) except that glucose was omitted. Cells were cultivated at 30°C in test tubes containing 5 ml of medium or in 2-liter flasks containing 500 ml of medium with reciprocal shaking (300 rpm for test tubes and 100 rpm for flasks).

To isolate bacteria which could desulfurize DBT in petroleum, several soil samples from various areas in Japan were transferred to test tubes containing medium A-1 supplemented with 5.4 mM DBT as a sole source of sulfur and 0.5% TD. Single colony isolation was repeated on the same medium containing agar. Among the DBT-utilizing strains in the presence of TD, we selected strain H-2.

Strain H-2 was cultivated in medium A-1 with 0.5% glucose and 0.27 mM DBT in 2-liter flasks for 2 days. Cells were harvested at 4°C by centrifugation at 10,000 x g for 15 min, washed once with 0.85% NaCl and resuspended in the same solution. The suspension was lyophilized and kept at -20°C until use. The reaction mixture contained, in 1 ml, TD, DBT which was dissolved in TD, 0.1 M potassium phosphate buffer (pH 7.0) and lyophilized cells. The reaction proceeded in test tubes at 30°C with reciprocal shaking (300 rpm).

DBT and 2-HBP were determined by gas chromatography or high performance liquid chromatography as described (10). TD was measured by gas chromatography under the same conditions. When the strain was cultivated in the medium with hydrocarbon, the cells floated on the surface of the medium. Therefore, growth could not be measured turbidimetrically. We centrifuged the culture broth at 15,000 x g for 45 min and the cell pellet was resuspended in 0.85% NaCl containing 5% polyoxyethylene lauryl alcohol ether (Brij 35). Cell growth was determined by measuring the optical density of this suspension. OD660 was proven to be proportional to the number of viable cells.

## RESULTS AND DISCUSSION

### Characterization of a DBT-utilizing bacterium in the presence of hydrocarbon

Among the isolates, a strain designated H-2 utilized DBT most rapidly in the presence of TD. The taxonomic properties were examined at the National Collection of Industrial and Marine Bacteria Ltd. (Aberdeen, Scotland, United Kingdom). As a result, the strain was identified as *Rhodococcus erythropolis*. There are some differences between our previous strain D-1 (10) and the present strain H-2 grown on carbon source such maltose, L-tyrosine and D-mannose: in strain H-2, these were possibly positive. Since this strain assimilated TD as a carbon source in addition to DBT as a sulfur source, several hydrocarbons were investigated to determine whether or not they could support the growth of *R. erythropolis* H-2. As shown in Table 1, this strain grew on n-alkanes with carbon chains longer than C8 with and without glucose, whereas it did not grow on n-hexane, styrene, p-xylene, cyclooctane and toluene even in the presence of glucose.

### Growth of *R. erythropolis* H-2 in the medium containing DBT and TD

The strain was cultivated in medium A-1 with TD as a sole source of carbon and DBT as a sole source of sulfur. The strain showed maximal growth (OD660=ca. 3.0) after 2 days of cultivation. DBT completely disappeared before this point. The metabolite 2-HBP was formed from DBT and it was almost equimolar to the amount of DBT degraded. The level of TD decreased slightly, and the pH decreased concomitantly with the increase of cell growth.

### DBT degradation by whole cell reactions

To prepare whole cells for DBT degradation, *R. erythropolis* H-2 was cultivated in medium containing either 0.5% glucose or 0.5% TD as a carbon source. Cells were lyophilized after harvesting and used for each reaction by resting cells. When the whole cell reactions proceeded with 50% TD for 4 h, the DBT degradation rates by cells pregrown in glucose and TD were 60 and 33%, respectively. Therefore, the following studies of whole cells reactions were performed using cells grown in glucose. DBT degradation was investigated using various amounts of lyophilized cells. The reaction proceeded most efficiently when the cells were added to the reaction mixture at a concentration of 80 mg/ml. However, DBT degradation was suppressed in the reaction mixture at elevated concentrations of the lyophilized cells. The limitation of oxygen may lower DBT degradation as found in *R. erythropolis* D-1 (10). DBT degradation in reaction mixtures containing various amounts of TD or DBT were examined. The reaction proceeded more efficiently with, than without TD. Even with as much as 70% TD, the degradation was enhanced compared with the situation without TD. The optimal concentration of TD was about 40%. TD at a concentration higher than 80% suppressed the degradation. In a reaction mixture supplemented with 40% TD and 80 mg/ml of the lyophilized cells, DBT up to 3 mM was completely degraded within 4 h. Figure 2 shows the time course of DBT degradation and 2-HBP accumulation. The amount of 2-HBP formed was almost stoichiometric to that of DBT degraded. It seemed that the level of TD was slightly decreased.

### Degradation of DBT and its derivatives by whole cell reactions

*R. erythropolis* H-2 was cultured in medium AG with DBT or its derivatives (Fig. 3) as the sole source of sulfur at 50 mg/l. The strain grew more or less on the four aromatic sulfur compounds tested: Growth (OD660) on DBT, 2,8-dimethyldibenzothiophene (2,8-dimethylDBT), 4,6-dimethyldibenzothiophene (4,6-dimethylDBT) and 3,4-benzodibenzothiophene (3,4-benzoDBT) in 4-day culture: 5.7, 4.7, and 1.7, respectively. Though 3,4-benzoDBT was not a good sulfur source for this strain, the two dimethylDBTs as well as DBT also supported the growth of this strain.

The reaction using lyophilized cells cultured with DBT, proceeded with DBT derivatives at 1 mM in the presence of TD. New peaks appeared on all the elution HPLC profiles with concomitantly decreasing substrate peaks. When DBT, 3,4-benzoDBT, 2,8-dimethylDBT, and 4,6-dimethylDBT were the substrates, the retention times of the new peaks were 3.5, 5.2, 4.6, and 5.2 min, respectively. The new peak in the DBT reaction profile corresponded to 2-HBP. The products in the reaction mixture using 2,8-dimethylDBT and 4,6-dimethylDBT as substrates were analyzed by gas chromatograph-mass spectrometry. Mass ions at  $m/z$  198 corresponding to the molecular mass of monohydroxy dimethylbiphenyls were detected. With 3,4-benzoDBT, the mass ion of the product at  $m/z$  220 was also obtained. These results indicated that the microbial desulfurization of these DBT derivatives and of DBT proceeded in a similar manner and gave the corresponding hydroxylated biphenyls as products. And it was interesting to know whether the hydroxy group of the 3,4-benzoDBT product was attached to the benzene, or the naphthalene ring. To identify their exact structures, the products from 3,4-benzoDBT, 2,8-dimethyl DBT and 4,6-dimethylDBT were purified from the reaction mixtures and analyzed by NMR.

In the case of 3,4-benzoDBT, signals were observed at  $\delta$  5.54 (s, 1 H), 7.04-7.09 (m, 1 H), 7.13 (d, 2 H,  $J=7.5$ ), 7.24-7.25 (m, 1 H), 7.26-7.27 (m, 2 H), 7.29-7.30 (m, 1 H), 7.33 (d, 1 H,  $J=8.2$ ), 7.35-7.36 (m, 1 H), 7.65 (d, 1 H,  $J=8.0$ ), and 8.51 (d, 1 H,  $J=8.2$ ). Since the signals at 7.07, 7.13 and 7.26 ppm were specific for one substituted benzene and those at 7.24 and 7.33 ppm were specific for 1,2,3,4-substituted benzene, this spectrum suggested that the hydroxy group is attached to the naphthalene ring. Therefore, we proposed that the structure of the product from 3,4-benzoDBT is a-hydroxy-b-phenylnaphthalene (Fig. 4).

The NMR signals in the case of 2,8-dimethylDBT and 4,6-dimethylDBT were assigned to 2-hydroxy-5,5'-dimethylbiphenyl and 2-hydroxy-3,3'-dimethylbiphenyl, respectively.

The amounts of products formed by whole cells were tentatively calculated assuming that the peak areas per mole of each product on the HPLC were the same as that of 2-HBP. Each substrate was thus converted to the corresponding product. The initial rates of degradation and desulfurization of 2,8-dimethylDBT, 4,6-dimethylDBT and 3,4-benzoDBT were about 120, 60, 20% that of DBT. The 2,8- and 4,6-dimethylDBTs were completely degraded within 6 h. *Arthrobacter* sp. readily attacked the sterically hindered 4,6-diethylDBT (18). Generally, there seems to be no steric hindrance of such alkyl groups against these enzyme systems. The chemical desulfurization rate for alkyl-substituted DBTs is much slower than that for DBT and it has been thought that the desulfurization of alkyl-substituted DBTs would also be less easy than that of DBT. Thus, these results indicate the feasibility of the practical microbial desulfurization of petroleum.

Although 3,4-benzoDBT was degraded slowly, the amount of the substrate was reduced to 0.1 mM after 12 h (Fig. 5). As described above, NMR analysis indicated that the hydroxy group of the identified product was attached to the naphthalene ring. These results suggest that the enzyme system involved in the microbial DBT desulfurization could distinguish between two carbon-sulfur bonds of 3,4-benzoDBT. The steric hindrance caused by the naphthalene ring might lead to this specificity.

Thus, the present work demonstrated that a new strain, identified as *R. erythropolis* H-2, utilized DBT as a sole source of sulfur and converted it to 2-HBP stoichiometrically even in the presence of hydrocarbon. This strain grew well in n-alkanes with relatively long carbon chains but not in hydrocarbons with higher toxicity to the organism such as toluene. The limiting log P value for the growth of our isolated strain was about 4.9 (log P value of n-octanol). From other experimental data (19), *R. erythropolis* H-2 revealed high tolerance against solvents compared with other Gram-positive bacteria, but it had less tolerance than Gram-negative bacteria such as *Pseudomonas* strains. Also in the whole cell reactions, DBT degradation proceeded in the presence of hydrocarbon and was enhanced by adding TD. TD may facilitate contact between DBT and cells since DBT is water immiscible.

The present strain was also found to have an ability to efficiently function in the presence of hydrocarbon and desulfurize DBT and DBT derivatives to form 2-HBP and the corresponding hydroxylated biphenyls, respectively. Therefore, the strain should be useful for the practical microbial desulfurization of petroleum.

**ACKNOWLEDGMENTS.** A part of this work has been conducted by the support of the Petroleum Energy Center (PEC) subsidized from Ministry of International Trade and Industry, Japan.

## REFERENCES

- (1) Klibane II, J.J. and Bielaga, B.A., Toward sulfur-free fuels. *CHEMTECH*, **20**:747-751 (1990).
- (2) Kodama, K., Nakatani, S., Umehara, K., Shimizu, K., Minoda, Y., Yamada, K., Identification of products from dibenzothiophene. *Agric. Biol. Chem.*, **34**:1320-1324 (1970).
- (3) Laborde, A.L. and Gibson, D.T., Metabolism of dibenzothiophene by a Beijerinckia species. *Appl. Environ. Microbiol.*, **34**:783-790 (1977).
- (4) Monticello, D.J., Bakker, D., and Finnerty, W.R., Plasmid-mediated degradation of dibenzothiophene by *Pseudomonas* species. *Appl. Environ. Microbiol.*, **49**:756-760 (1985).
- (5) Crawford, D.L. and Gupta, R.K., Oxidation of dibenzothiophene by *Cunninghamella elegans*. *Curr. Microbiol.*, **21**:229-231 (1990).
- (6) Afferden, M. van, Schacht, S., Klein, J., and Truper, H.G., Degradation of dibenzothiophene by *Brevibacterium* sp. DO. *Arch. Microbiol.*, **153**:324-328 (1990).
- (7) Klibane II, J.J. and Jackowski, K., Bidesulfurization of water-soluble coal-derived material by *Rhodococcus rhodochrous* IGTS8. *Biotechnol. Bioeng.*, **40**:1107-1114 (1992).
- (8) Omori, T., Monna, L., Saiki, Y., and Kodama, T., Desulfurization of dibenzothiophene by *Corynebacterium* sp. strain SY1. *Appl. Environ. Microbiol.*, **58**:911-915 (1992).
- (9) Olson, E.S., Stanley, D.C., and Gallagher, J.R., Characterization of intermediates in the microbial desulfurization of dibenzothiophene. *Energy & Fuels*, **7**:159-164 (1993).
- (10) Izumi, Y., Ohshiro, T., Ogino H., Hine, Y., and Shima, M., Selective desulfurization of dibenzothiophene by *Rhodococcus erythropolis* D-1. *Appl. Environ. Microbiol.*, **60**:223-226 (1994).
- (11) Ohshiro, T., Hine, Y., and Izumi, Y., Enzymatic desulfurization of dibenzothiophene by a cell-free system of *Rhodococcus erythropolis* D-1. *FEMS Microbiol. Lett.*, **118**:341-344 (1994).
- (12) Gallagher, J.R., Olson, E.S., and Stanley, D.C., Microbial desulfurization of dibenzothiophene: A sulfur-specific pathway. *FEMS Microbiol. Lett.*, **107**:31-36 (1993).
- (13) Kayser, K.J., Bielaga-Jones, B.A., Jackowski, K., Odusan, O., and Klibane II, J.J., Utilization of organosulfur compounds by axenic and mixed cultures of *Rhodococcus rhodochrous* IGTS8. *J. Gen. Microbiol.*, **139**:3123-3129 (1993).
- (14) Wang, P. and Krawiec, S., Desulfurization of dibenzothiophene to 2-hydroxybiphenyl by some newly isolated bacterial strains. *Arch. Microbiol.*, **161**:266-271 (1994).
- (15) Denome, S.A., Olson, E.S., and Young, K.D., Identification and cloning of genes involved in specific desulfurization of dibenzothiophene by *Rhodococcus* sp. strain IGTS8. *Appl. Environ. Microbiol.*, **59**:2837-2843 (1993).
- (16) Denome, S. A., Oldfield, C., Nash, L. J., and Young, K. D., Characterization of desulfurization genes from *Rhodococcus* sp. strain IGTS8. *J. Bacteriol.*, **176**:6707-6716 (1994).
- (17) Piddington, C. S., Kovacevich, B. R., and Rambosek, J., Sequence and molecular characterization of a DNA region encoding the dibenzothiophene desulfurization operon of *Rhodococcus* sp. strain IGTS8. *Appl. Environ. Microbiol.*, **61**:468-475 (1995).
- (18) Lee, M. K., Senius, J. D., and Grossman, M. J. Sulfur-specific microbial desulfurization of sterically hindered analogs of dibenzothiophene. *Appl. Environ. Microbiol.*, **61**:4362-4366 (1995).
- (19) Inoue A, Horikoshi K, Estimation of solvent-tolerance of bacteria by the solvent parameter Log P. *J. Ferment. Bioeng.*, **71**:194-196 (1991).

TABLE 1. Growth in the presence of hydrocarbons. The strain was cultivated in medium A-1 with 0.5% hydrocarbons with or without 0.5% glucose in test tubes for 4 days.

Hydrocarbon	(log <i>P</i> value)	+Glucose		-Glucose	
		Growth (OD660)	pH	Growth (OD660)	pH
None		4.8	4.6	n.t. <sup>a)</sup>	n.t. <sup>a)</sup>
<i>n</i> -Hexadecane	(7.0<)	4.9	4.2	5.2	5.1
<i>n</i> -Tetradecane	(7.0<)	5.6	3.8	4.9	3.8
<i>n</i> -Dodecane	(7.0)	2.9	4.2	3.0	4.8
<i>n</i> -Decane	(6.0)	1.7	5.7	2.5	6.4
<i>n</i> -Nonane	(5.5)	0.8	5.7	0.8	5.8
<i>n</i> -Octane	(4.9)	0.3	6.5	0.3	6.6
Cyclooctane	(4.5)	0	6.9	0	6.9
<i>n</i> -Hexane	(3.9)	0	7.0	0	6.9
<i>p</i> -Xylene	(3.1)	0	7.0	0	7.0
Styrene	(2.9)	0	6.9	0	6.9
Toluene	(2.8)	0	6.9	0	7.0

a) not tested

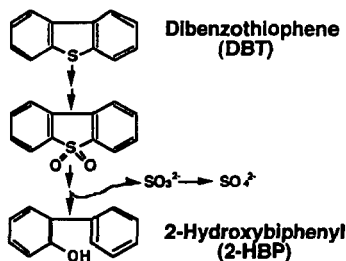


FIGURE 1. Proposed sulfur-specific pathway of dibenzothiophene (DBT)

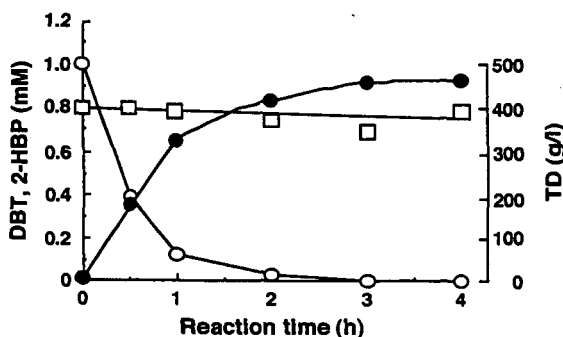


Figure 2. Time course of DBT degradation and 2-hydroxybiphenyl (2-HBP) accumulation in the whole cell reaction.  $\circ$  DBT,  $\bullet$  2-HBP,  $\square$  TD

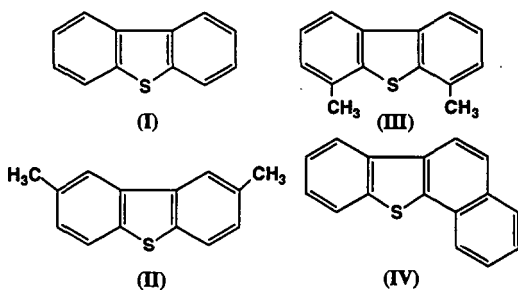


FIGURE 3. Structure of DBT and its derivatives. (I) DBT; (II) 2,8-dimethylDBT; (III) 4,6-dimethylDBT; (IV) 3,4-benzoDBT.

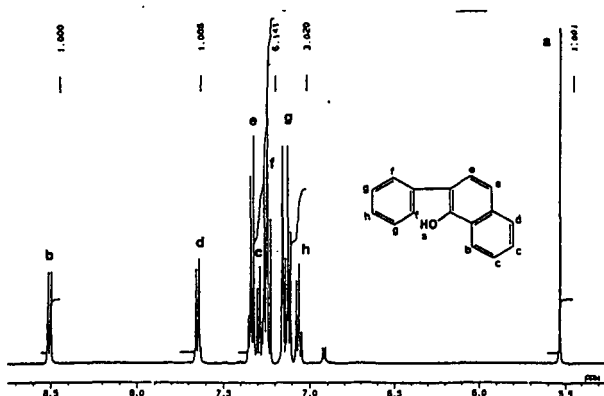


FIGURE 4. <sup>1</sup>H-NMR spectrum of the product from 3,4-benzoDBT.

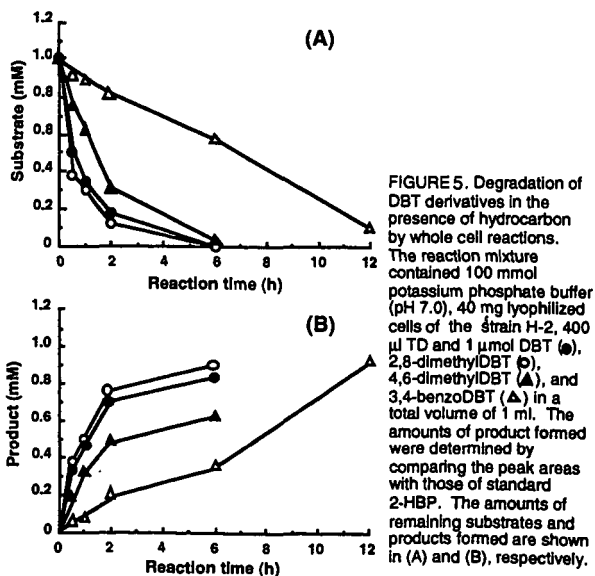


FIGURE 5. Degradation of DBT derivatives in the presence of hydrocarbon by whole cell reactions. The reaction mixture contained 100 mmol potassium phosphate buffer (pH 7.0), 40 mg lyophilized cells of the strain H-2, 400  $\mu$ l TD and 1  $\mu$ mol DBT (●), 2,8-dimethylDBT (◐), 4,6-dimethylDBT (◑), and 3,4-benzoDBT (Δ) in a total volume of 1 ml. The amounts of product were determined by comparing the peak areas with those of standard 2-HBP. The amounts of remaining substrates and products formed are shown in (A) and (B), respectively.

# ANALYSIS OF THE EXTENT OF SULFUR REMOVAL AND THE EFFECT ON REMAINING SULFUR

M. K. Lee, R. C. Prince, J. D. Senius, M. J. Grossman  
Exxon Research and Engineering Co., Annandale, NJ 08801

I. J. Pickering, G. N. George  
SSRL, Stanford, CA 94309

Keywords: Biodesulfurization, middle distillate, vacuum gas oil

## INTRODUCTION

Hydrodesulfurization (HDS) is used to remove organic sulfur from petroleum oils in the refining process. DBTs bearing alkyl substitutions adjacent to the sulfur atom (referred to as sterically hindered compounds), are the most resistant to HDS, and represent a significant barrier to reaching very low sulfur levels in fuels<sup>1</sup>. Bacteria have been isolated which utilize an oxidative pathway to selectively desulfurize a variety of organic sulfur compounds found in petroleum oils<sup>2</sup>. The molecular mechanisms of dibenzothiophene (DBT) desulfurization by this pathway have recently been described<sup>3</sup>. Previous experiments with *Rhodococcus* sp. ECRD-1 (ATCC 55309) using DBT have shown that it is converted to the hydroxylated sulfur-free end product 2-phenylphenol via an analogous pathway<sup>4</sup>. Corresponding conversions of the sterically hindered compounds 4,6-diethyl DBT, 4,6-dimethyl DBT and 4-ethyl DBT were also demonstrated.

This study evaluates the ability of ECRD-1 to desulfurize feeds encountered in refineries and examines the fate of sulfur remaining in the oil. A middle distillate oil (232 - 343°C) and a vacuum gas oil (VGO) (343 - 496°C), representing a diesel range oil and a heavy gas oil, were tested as sole sulfur sources in batch cultures. Sulfur removal was quantified using the ratio of Flame Ionization (FID) and Sulfur Chemiluminesce (SCD) detector response factors in Gas Chromatography analysis. Results demonstrated that up to 40% of sulfur in the middle distillate cut could be removed in two week batch cultures. Compounds across the entire boiling range of the oil were affected by the treatment. Less than half that removal is evident in the heavier VGO, suggesting limitations on the range of compounds susceptible to desulfurization by this system. Analysis of the chemical state of the sulfur remaining in the treated oils by sulfur K-edge X-ray absorption spectroscopy showed that in the case of the middle distillate oil over 50% of the remaining sulfur was in an oxidized form. A lesser amount of the remaining sulfur in the treated VGO was in an oxidized state, consistent with the degree of desulfurization. The presence of partially oxidized sulfur compounds in the treated oils indicates that these compounds were en route toward desulfurization. Overall, in the case of the middle distillate oil, more than two-thirds of the initial sulfur had been affected by the microbial treatment.

## EXPERIMENTAL

**Bacterial Strain.** *Rhodococcus* sp. ECRD-1 (ATCC 55309), previously designated *Arthrobacter* sp. D-1 (ATCC 55309), was isolated by enrichment culture from marine sediments based on its ability to selectively remove sulfur from the sterically hindered organic sulfur compound 4,6-DEDDBT<sup>1</sup> using the organic sulfur compound as a sole sulfur source.

**Media.** Mineral Salts Sulfur-Free Medium (MSSF) containing 1% sodium acetate was prepared as previously described<sup>1</sup> and used for oil desulfurization experiments. Tungsten was added as 50 ug/ml Na<sub>2</sub>WO<sub>4</sub> · 2H<sub>2</sub>O in VGO cultures. Sulfate control media contained 0.2 g MgSO<sub>4</sub> · 7H<sub>2</sub>O per liter.

Luria broth (LB) was used to grow cultures for use as and contained per liter: 10 g Difco tryptone, 5 g Difco yeast extract, 5 g NaCl, adjusted to pH 7.0 with 1.0 ml 1 M NaOH and autoclaved at 121°C, 15 psi.

**Oils.** Oregon Basin (OB) crude oil, a 450 - 650°F (232 - 343°C) middle distillate cut, represents a diesel range oil fraction. The OB oil used for experiments was artificially weathered under a stream of nitrogen to a constant weight to eliminate inconsistencies caused by evaporative loss of oil during culturing or extraction. Weathering resulted in a weight loss of less than 10% and no change in ppm sulfur content. Vacuum gas oil (VGO), a 650 - 950°F (343 - 496°C) distillate cut, represents a heavy oil fraction. The oil used was also artificially weathered under a stream of nitrogen to a constant weight to eliminate inconsistencies caused by

untreated oils was determined by X-ray fluorescence sulfur analysis (XRF) and GC/FID/SCD. The percent sulfur for the Oregon Basin cut sterile control was 2.07% determined by XRF and 1.96 % by GC/FID/SCD. The percent sulfur for the VGO cut sterile control was 2.93% determined by XRF and 2.26% by GC/FID/SCD.

**Biodesulfurization Assays.** Biodesulfurization were performed as growing cell assays. One ml, approximately 0.84 g, of artificially weathered and heat sterilized oil was treated in one liter of culture. Inocula were prepared from overnight cultures grown from single bacterial colonies in LB at room temperature (23°C) on a VWR Orbital shaker at 200 rpm. Cells were then pelleted in a Sorval centrifuge at 3000 x g in SS34 rotor at 4°C. The pellet was washed three times with one volume of 12 mM phosphate buffer (pH 7.0) previously chilled on ice for 30 min. Cell pellets were resuspended in 1/10 the original culture volume of chilled phosphate buffer and used immediately for inoculation. Flasks were inoculated with 2 ml of the cell suspension per L medium.

Duplicate cultures were incubated with shaking at 200 rpm for 4 days for OB oils. The experiment also included a uninoculated negative control. VGO oils were incubated with shaking at 200 rpm for 5 and 7 days. The five day experiment included a positive control culture, inoculated and containing sulfate. The seven day experiment included a uninoculated negative control. Flasks were pH monitored at one to two day intervals and adjusted to pH 7.0 with 1M phosphoric acid when the pH deviated by more than 1.0 pH unit. All assays were performed in duplicate.

Before extraction, cultures were brought to a pH of 1.0 with 1N HCl. A 0.5 ml aliquot of 1% v/v dodecane in methylene chloride solution was added as an extraction standard. Each flask was then extracted 3X with 100 ml methylene chloride. The methylene chloride extracts were filtered through anhydrous sodium sulfate or calcium sulfate if water was apparent (i.e., a turbid solution was observed). The samples were then reduced to approximately 5 ml volumes under nitrogen. Samples were subsequently filtered through a 0.22 µm hydrophobic filter to remove turbidity (attributed to water condensate) appearing after volume reduction. For every liter of culture extracted, a 0.5 ml aliquot of decane/methylene chloride (0.742 g/100 ml) was added to the filtered extracts as an injection volume standard. The solutions were then concentrated to approximately 1.0 ml.

**GC/FID/SCD Analysis.** Gas Chromatography was performed on a Perkin-Elmer GC Autosystem (split/splitless injector). Oregon Basin oil was chromatographed on a Supelco SPB-1 column (30m x 0.32mm, 0.25µm film thickness). The temperature zones for the GC were as follows: injector and detector temperature 300°C, initial oven temperature 40°C for 1 minute, followed by a 4°C/minute temperature ramp to 300°C for a final 10 minute hold. VGO was chromatographed on a Supelco SPB-1 column (15 m x 0.32mm, 4µm film thickness). The temperature zones for the GC were as follows: injector temperature 275°C, detector temperature 325°C, initial oven temperature 50°C for 1 minute, followed by a 5°C/minute temperature ramp to 300°C for a final 20 minute hold. Tandem Perkin-Elmer FID (flame ionization detection) and Sievers Instruments, model 355 SCD (sulfur chemiluminescence detection) detectors were used to determine sulfur concentrations in oil samples based on response factors of model compounds. For oils and standard mixtures, 1 µl of sample was injected in duplicate and results averaged.

Response factors for OB oil and VGO were estimated based on the averaged FID and SCD response factors for a number of model compounds. These compounds were chosen to represent some of the compounds found in the oils. The standards used for calibration of the FID detector were hexane, heptane, decane, dodecane, tetradecane, fluorene, carbazole, DBT sulfone, and 4,6 DEDBT. The sulfur compounds contained in this mixture were used to calibrate the SCD. Averaged response factors for sulfur (ng/area) and for carbon (mg/area) were calculated for the standard mixtures and the sulfur/carbon ratio calculated. This ratio was multiplied by the sulfur/carbon area of the oils to give ppm S. A common baseline was drawn by the computer encompassing all area associated with the oil so that unresolved area characterized by a hump in the baseline was included in subsequent calculations.

The percent carbon loss for treated oils was determined as the difference between the GC/FID area ratio of total carbon (minus standards) to dodecane extraction standard of control and treated samples.

**Sulfur K-edge X-ray absorption-edge spectroscopy.** Sulfur K-edge X-ray absorption-edge spectroscopy was used to determine the effect of biodesulfurization on the remaining sulfur content of treated oils. This technique allows for the evaluation of the chemical state of sulfur

Stanford Synchrotron Radiation Laboratory. Reference compounds were run as powder films using electron yield detection, while oil samples were run as liquids using fluorescence detection<sup>2</sup>. Spectra of the oils were fitted to linear combinations of the spectra of reference compounds using least-squares non-linear optimization<sup>3</sup>. In general there is a trend toward higher absorbance energies in the order sulfidic, thiophenic, oxidized species (Fig. 1).

The procedure employed to fit the oil spectra employed a fairly broad range of model organic sulfur compounds as reference compounds to represent the majority of sulfur types expected in treated and untreated oils. Fig. 1 shows the sulfur K-edge X-ray absorption spectra of these compounds. Although the individual spectra are quite distinct, different fit results were obtained with good fits using different constraints on the fit calculations. Consequently, the fits obtained using this method are used as indicators of the likely distribution of S compounds and are not considered highly accurate for specific species.

## RESULTS AND DISCUSSION

**Oregon Basin Oil.** The desulfurization of OB oil ECRD-1 cultures grown for four days resulted in a large reduction in sulfur containing compounds. The GC/SCD chromatograms for a sterile control and ECRD-1 desulfurized oil show that sulfur components across the entire boiling range of the oil were effected (Fig. 2). The total sulfur removed was 35 ( $\pm$  30% RSD). Examination of the GC/FID profile (Fig. 3) revealed a reduction in the resolved peaks (n-alkanes) in the treated cultures. Loss of the straight chain hydrocarbons is attributed to degradation by ECRD-1 which is known to degrade these compounds. The loss of carbon in these samples was averaged 26% ( $\pm$  7% RSD). Taking into account the consumption of carbon, the reduction of sulfur the maximum sulfur removed is calculated to be 58%.

Analysis of the oils by sulfur K-edge X-ray absorption-edge spectroscopy was performed to determine the effect of treatment on the remaining sulfur in the oil. The sulfur spectra of the treated, sterile control and original oils are shown in Fig. 4. The spectra of the weathered OB oil and the sterile control are virtually identical indicating no abiological effects occurred due to the culture conditions used. In contrast, the spectrum of the treated oil is markedly different, showing an increase in absorbance at approximately 2473 and 2477 eV. A shift in absorbance toward higher energies (eV) is characteristic of more oxidized sulfur species, (see Fig. 1), indicating that a significant proportion of the sulfur compounds remaining in the oil contain sulfur in an oxidized form.

Table 1 shows the best fit composition of sulfur forms in the sterile and treated oil. A small feature near 2480 eV was observed for both samples and is attributed to sulfate contaminating the graphite used for sample preparation.

**Vacuum Gas Oil.** Cultures of ECRD-1 grown on VGO as the sole sulfur source for five and seven days showed growth and sulfur reduction. The inoculated positive control containing sulfate also showed growth but no sulfur removal. The negative controls showed no growth. After incubation the concentration of sulfur in the VGO in the positive control and the sterile control cultures were equivalent, both approximately 2.3%. The lack of desulfurization in the presence of sulfate is consistent with previous observations that sulfate represses the expression of desulfurization activity in ECRD-1 (Table 2). The 7 day ECRD-1 cultures showed a 16% sulfur reduction as compared to only 7% for the five day cultures. The difference in desulfurization levels demonstrates that additional desulfurization of VGO is achieved with extended incubation periods. However, in comparison to OB oil, VGO appears relatively more resistant to desulfurization by ECRD-1.

Analysis of the treated VGO samples by X-ray spectroscopy showed an increase in absorbance at approximately 2477 eV in all treated samples (Fig. 5). This increase in absorbance is consistent with the production of oxidized sulfur compounds, albeit considerably less than that observed with the OB oil. No changes in the spectrum were observed for the culture amended with sulfate (data not shown) corroborating the GC results and demonstrating that no detectable desulfurization activity occurred. Due to the relatively small change in the spectrum for the treated VGO the changes in oxidized species could not be meaningfully fit with model compounds.

## CONCLUSIONS

This study has shown that ECRD-1 can desulfurize complex sulfur found in a middle distillate cut and a vacuum gas oil. Consumption of hydrocarbons could impact negatively on process economics. However, there is no indication that hydrocarbon degradation is tied to desulfurization. Hydrocarbon degradation activity could be eliminated through genetic

microbial treatment, complete desulfurization was not achieved. However, a significant percentage of the remaining sulfur is oxidized by the treatment indicating the potential for further desulfurization. Additionally, the ability to remove sterically hindered compounds not affected by HDS could prove valuable.

- <sup>1</sup> Kabe, T., Ishihara, A. and Tajima, H. 1992. *Ind. Eng. Chem. Res.* **31**:1577-1580.
- <sup>2</sup> Grossman, M.J., in "Hydrotreating technology for pollution control: Catalysts, Catalysis, and Processes" (M. L. Occelli and R. Chianelli, eds.) Marcel Dekker, New York, pp. 345-359, 1996.
- <sup>3</sup> Gray, K.A., Pogrebinsky, O.S., Mrachko, G.T., Xi, Lei, Monticello, D.J., and Squires, C.H. 1996. *Nature Biotechnology* **14**:17051709.
- <sup>4</sup> Lee, M.K., Senius, J.D., and Grossman, M.J. *Appl. Environ. Microbiol.* **61**:4362-4366 (1995).
- <sup>5</sup> George, G.N., Gorbaty, M.L., Kelemen, S.R., and Sansone, M. *Energy & Fuels* **5**: 93-97 (1991).

Model compound	Relative % total S as this species	
	Sterile control (2.0% S)	ECRD-1 treated (1.1% S)
2,5 Dimethylthiophene	51	24
Benzyl sulfide	47	18
Dimethylsulfoxide	-	32
Dibenzothiophene sulfone	-	24
Sulfate	2	2

Sample	% Sulfur(±%RSD)	% S Removed
5 day culture Positive Control	2.27±4%	-
5 day culture ECRD-1 Treated	2.11±0.1%	7.0
7 day culture Negative Control	2.25±1%	-
7 day culture ECRD-1 Treated	1.91±3%	15.5

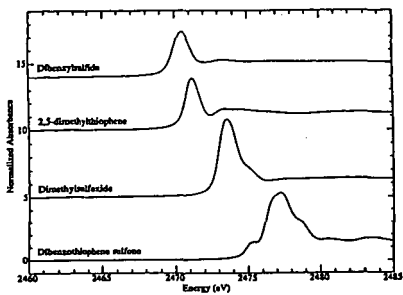


Figure 1. Sulfur K-edge X-ray Absorption Spectra of reference compounds.

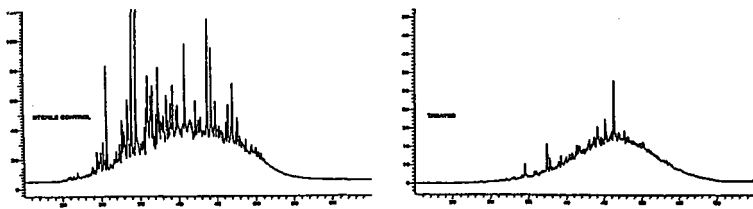


Figure 2. GC/SCD of sterile control and treated Oregon Basin oil.

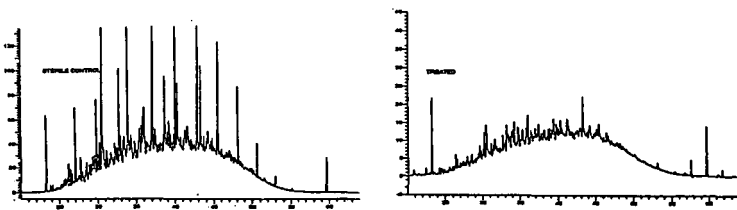


Figure 3. GC/FID of sterile control and treated Oregon Basin oil.

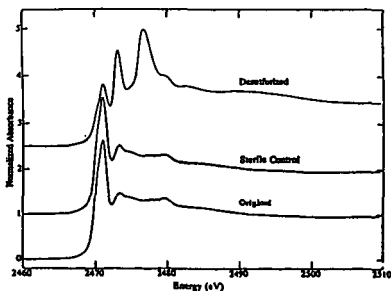


Figure 4. Sulfur K-edge X-ray absorption-edge spectra of original, sterile control and treated Oregon Basin Oil.

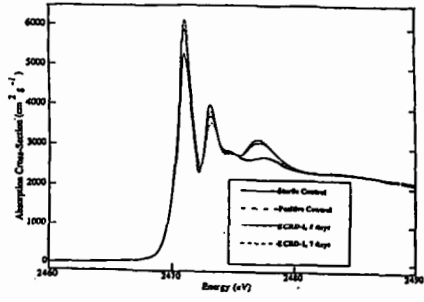


Figure 5. Sulfur K-edge X-ray Absorption spectra of Vacuum Gas Oil sterile control, positive control, and five and seven day ECRD-1 treatment

# AQUATHERMOLYSIS OF ORGANIC COMPOUNDS IN THE PRESENCE OF HYDROGEN SULFIDE AND SULFATE

Gerhard G. Hoffmann and Thorsten David  
German Petroleum Institute,  
Walther-Nernst-Str. 7  
Clausthal-Zellerfeld, G-38678  
Germany

**Keywords:** Thermochemical reduction of sulfate, formation and decomposition of organic sulfur compounds caused by aquathermolysis, hydrogen sulfide

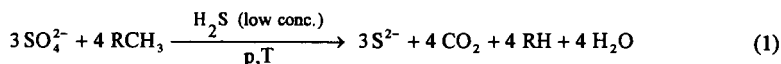
## ABSTRACT

Thermal recovery processes are well established enhanced oil recovery techniques. At thermal recovery temperatures in the reservoir can reach 320°C. Under these specific conditions chemical reactions of the reservoir sulfate and hydrogen sulfide easily occur. The conditions at thermal recovery processes allow the thermochemical reduction of sulfate with hydrogen sulfide. In the presence of organic compounds these redox reactions lead to the formation of a variety of inorganic, as well as organic compounds in different oxidation states, including elemental sulfur.

Object of these investigations was to study the thermal induced reactions of organic compounds in the presence of hydrogen sulfide and aqueous solutions of alkali metal- as well as alkaline-earth metal sulfates. *n*-Octane, *n*-hexadecane, and 2-octanone selected as representative organic compounds were allowed to react with the inorganic components in autoclaves at temperatures up to 320°C under variation of the reaction time from 6 hrs. to 500 hrs. The amount of reduced sulfate was estimated by quantitative determination of the residual sulfate in the aqueous layer after each reaction. The organic reaction products were identified by gas chromatography and GC/MS.

## INTRODUCTION

Thermal recovery processes are well established enhanced oil recovery techniques and widely applied for recovering heavy oil, heavy oil sands, and shale oil. At thermal recovery temperatures in the reservoirs can reach 320°C. Under these specific conditions decomposition reactions of organic sulfur compounds, which are already present in the crude oil, easily proceed. In addition, reactions of the reservoir sulfate and hydrogen sulfide (H<sub>2</sub>S) take place.[1] The conditions, occurring at thermal recovery processes allow the thermochemical reduction of sulfate with H<sub>2</sub>S. In the presence of organic compounds these redox reactions lead to the formation of a variety of inorganic and organic sulfur compounds in different oxidation states, including elemental sulfur (or its different radicals). The reduction is autocatalytic with respect to H<sub>2</sub>S. Increasing concentrations of elemental sulfur promptly cause its reaction with organic compounds of the crude oil, which consequently leads to the formation of organic sulfur compounds and H<sub>2</sub>S.[2-4] Thus, it is obvious that both, consumption and formation of H<sub>2</sub>S compete with each other. The net reaction can be given with eq.1:



From eq.1 it becomes evident that only a catalytic amount of H<sub>2</sub>S is necessary to initiate the thermochemical reduction of sulfate. It is known that H<sub>2</sub>S is very often present in the reservoir. It can be formed under fairly mild conditions by microbial reduction of sulfate.[5] Furthermore, H<sub>2</sub>S can be generated by the hydrolysis of inorganic compounds like pyrite, pyrotite, and elemental sulfur.

The pH-value plays an important part in the thermal reduction, since it has a significant influence on both, the formation and the reactivity of the inorganic sulfur compounds.[6] The pH-value is strongly controlled by the metal cation of the used sulfate solutions.

The net reaction (eq.1) reveals that sour gas (CO<sub>2</sub> + H<sub>2</sub>S) is formed. These compounds lead to severe problems at the recovery of crude oil, as well as at its manufacturing. Furthermore, the quality of the crude oil will be affected.[7] The changes in the composition of the hydrocarbons and heterocompounds due to aquathermolysis in the absence of sulfate and H<sub>2</sub>S are well described in literature.[8] However, only few details

concerning the very complex thermochemical reduction of sulfate in the presence of  $H_2S$  and hydrocarbons are available.[1,4,9] On the other hand, sulfate as an oxidizing agent for the synthesis of aromatic carboxylic acids, such as phthalic acids, has been earlier investigated.[10] Moreover, formation of  $H_2S$  from the reduction of gypsum has been subject of investigations.[11]

Scope of our research is to better understand the above mentioned reactions and their influences on each other with respect to the different reaction products, which are formed, depending on the reaction time, the reaction temperature, and the employed educts. The reactions were carried out in the presence of aqueous solutions of metal sulfates; moreover, in every reaction only one defined aliphatic hydrocarbon was used serving as a model compound; this was necessary to understand the complex reactions taking place.

## EXPERIMENTAL

The experiments were conducted using glass cylinders, which were installed in stainless steel autoclaves. In the case of the reactions with model compounds an aqueous solution of 20 mmol of the corresponding sulfate was used, whereas in the case of crude oil a solution containing 60 mmol of sulfate was employed. Autoclaves of 90 ml and 190 ml content, respectively, were used. Reactions with  $CaSO_4$  were carried out in the presence of  $NaH_2PO_4$  (employed in the same molar ratio as  $CaSO_4$ ). The starting pressure at ambient temperature was the steel cylinder pressure of  $H_2S$ . The reactions were performed at temperatures between 200°C and 320°C, respectively (Tab.1). After given time intervals the autoclave was cooled to room temperature (RT). The organic layer was separated from the aqueous layer. The decrease of sulfate was determined by quantitative titration, according to the method of SCHÖNINGER.[12] The pH-value of the aqueous phase was determined after the reaction at RT with a pH-meter equipped with a glass electrode. The organic layer was investigated by gas chromatography (GC) and the coupling of gas chromatography with mass spectrometry (GC/MS). GC was performed using a Hewlett Packard Model 5890 Series II instrument, equipped with a Hewlett Packard Flame Ionization Detector (FID) and a Hewlett Packard Photometric Detector (FPD). The organic layer was analyzed by GC/MS using a Hewlett Packard 5890 A Series II GC coupled with a Hewlett Packard 5970 B Series MS Detector, using the same GC program as for the separation. Mass spectra were obtained by electron ionization at 70 eV. The injector system of the GC/MS was a temperature programmable Injector System from Gerstel. The analytical conditions are given in Tab.2. Reactions in the presence of crude oil were worked up in the same manner. However, the recovered crude oil was extracted by liquid sulfur dioxide in order to enrich organic sulfur compounds.[13] The enriched crude oil fractions were investigated by GC (FID, FPD).

## RESULTS AND DISCUSSION

In Tab.1 the parameters of the performed reactions are summarized. To rule out artifacts and to make sure that sulfate does not react with the autoclave material, aqueous solutions of the investigated compounds were treated at elevated temperatures under helium or nitrogen pressure in stainless steel autoclaves without  $H_2S$  (Tab.1: 1-3). It could be proved that neither reduction of sulfate nor reaction of the organic compound takes place. Sulfate was recovered quantitatively, the organic compound unchanged.

In Fig.1 the amount of reduced sulfate of the reaction of different metal sulfates in the presence of *n*-octane (Fig.1; according to Tab.1: 4, 6-9, 13-17, and 23, 24) is plotted vs. the temperature. In these experiments the reaction time was 72 hrs. It easily can be seen that the reduction rate is strongly controlled by both, reaction temperature and metal cation of the employed sulfate. To attain the same rate of reduction reactions of  $MgSO_4$  require higher temperatures than those of  $CaSO_4/NaH_2PO_4$ . Generally, it can be seen from Fig.1 that the rate of reduction strongly increases at temperatures higher than 250°C. The strong influence of the employed cation becomes evident by comparing the reactions of  $Na_2SO_4$  to those of  $Al_2(SO_4)_3$ . In the case of sodium sulfate reduction is not as pronounced; after a reaction time of 500 hrs. only about 10% of  $Na_2SO_4$  are reduced at 320°C (Tab.1: 4, 5). In contrast, the reduction in the presence of aluminum ions already starts at 100°C and is almost quantitative at 200°C (Tab.1: 22-24).

In Fig.2 the amount of reduced sulfate of the reactions in the presence of *n*-octane is plotted vs. the reaction time (Fig.2; according to Tab.1: 4, 9-12, 17-21, 24, 25). In this case, the reaction temperature was 320°C. It can be seen from the plots of  $MgSO_4$  and  $CaSO_4/NaH_2PO_4$  that the rate of reduction increases with increasing reaction time. It is reaching 97% within 144 hrs. for  $MgSO_4$ ; whereas for  $CaSO_4/NaH_2PO_4$  only 88% of the

sulfate is reduced within the same reaction time. This indicates that the reaction is controlled by the cation, too; this feature becomes very evident for the reactions of  $\text{Al}_2(\text{SO}_4)_3$  and  $\text{Na}_2\text{SO}_4$ . In the presence of aluminum cations the reduction of sulfate proceeds very fast (see for example Tab.1: 25), whereas the reactivity is very low in the presence of sodium cations (Tab.1: 4, 5). An explanation can be given with the pH-value.

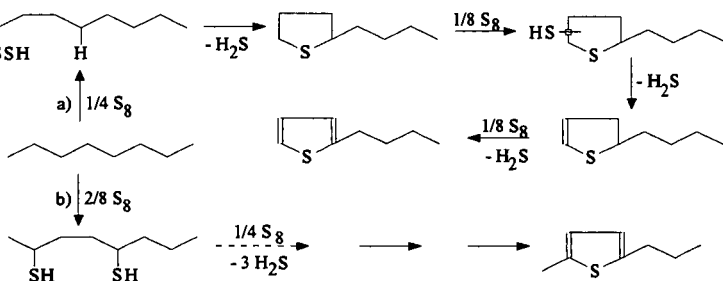
By comparison of the experiments 9, 26, and 27 (Tab.1) it becomes evident that the rate of reduction of sulfate does not only depend on the reaction time and the reaction temperature; it is also influenced by the organic compound which is involved in the reaction. In the presence of *n*-octane 66% of the employed  $\text{MgSO}_4$  is reduced; whereas in the presence of *n*-hexadecane or 2-octanone the rate of reduction increases significantly to approximately 80%.

Experiments 28 to 30 (Tab.1) confirm that in the presence of crude oil the rate of reduction of sulfate lies in a similar order of magnitude.

Investigations of the organic layer reveal that preferably organic sulfur compounds are formed. A strong influence of the employed metal salt on the distribution of the different newly formed organic compounds could be shown. Moreover, the reaction conditions, e.g. reaction temperature, as well as time are of main importance.

In Figures 3 to 6 an example of the identification steps of the organic compounds is given. Fig.3 shows the FID chromatogram of the organic layer of reaction 9 (Tab.1); in Fig.4 the corresponding FPD chromatogram is shown. The two chromatograms reveal that a lot of organic compounds are newly formed. In addition, the FPD chromatogram indicates that many organic sulfur compounds are generated. Most of these compounds can be assigned to mono-, as well as dialkylated thiophenes by GC/MS. Moreover, a compound containing two sulfur atoms is observed; 2,2'-bithiophene could be made plausible. The ion chromatogram of the ion mass 111 is shown in Fig.5. It can be seen that a great number of different compounds is formed, the fragmentation of which leads to ion mass 111. Mass 111 is e.g. specific for dialkylated thiophenes containing at least one methylgroup as ring substituent. By comparing the single mass spectra of the total ion current to literature data a specification of 2,5- and 2-alkylsubstituted thiophenes becomes possible. Fig.6 shows one specific example for a typical mass spectrum; it could be shown that 2-ethyl-5-methylthiophene corresponds to this particular spectrum.

The tentative overall reaction is shown in Scheme 1. It can be assumed that at the reduction of sulfate sulfur radicals are generated; these radicals subsequently react with *n*-alkanes as shown in Scheme 1a and 1b, respectively:



Scheme 1.

A series of insertion reactions of sulfur into carbon hydrogen bonds of the alkane, followed by a condensation reaction in the 2,5-position, as well as in the 1,4-position of the alkane lead to ring closure. Thus, 2,5-substituted and 2-substituted tetrahydrothiophene derivatives are formed. Under elimination of  $\text{H}_2\text{S}$  cyclisation may proceed as shown in Scheme 1a or 1b. The thus formed tetrahydrothiophene derivatives react in a cascade of sulfur insertion, as well as  $\text{H}_2\text{S}$  elimination steps to form the corresponding thiophenes.

In addition, other than sulfur containing compounds are formed, too. Some of these could be identified by GC/MS as ketones, e.g. 2-, 3-, and 4-octanone and aromatic compounds, like benzene and ethylbenzene.

Some of the reaction products of experiments 9, 26, and 27 (Tab.1) are identified following published sources [14] and are summarized in Tab.3. The formation of typical

classes of organic compounds, such as substituted thiophenes, ketones and aromatic compounds is clearly indicated.

Furthermore, the GC- and GC/MS-spectra reveal a successive degradation of the alkyl substituents with increasing reaction time and increasing reaction temperature; a tentative overall reaction is already given elsewhere.[4]

## CONCLUSIONS

In autoclave experiments the thermal reduction of sulfate in the presence of small amounts of H<sub>2</sub>S and aliphatic organic compounds leads to the formation of a great number of organic compounds; many of these contain sulfur as a heteroatom. Alkyl substituted thiophenes are formed in substantial amounts. Evidence is given that the degradation of the alkyl substituents proceeds to form carbon dioxide.

The results of these investigations demonstrate that the conditions at thermal recovery of crude oil are responsible for thermochemical reduction of sulfate. This reaction is catalyzed by H<sub>2</sub>S. Inorganic sulfur compounds in different oxidation states, such as elemental sulfur are formed and react with hydrocarbons of the reservoir. These reactions lead to the formation of typical types of organic compounds, such as alkyl substituted thiophenes, ketones, and aromatic compounds, respectively. Thus, at thermal recovery a rapid alteration of crude oil becomes possible and subsequently has a main impact on the quality of the recovered crude oil, as well as the quality of the reservoir.

## ACKNOWLEDGMENTS

We thank the Fond der Chemischen Industrie for financial support. T.D. thanks the German Petroleum Institute for a scholarship within the BMBF program of HSP II.

## REFERENCES

- [1] a) Orr, W.L., *Am. Ass. Pet. Geol. Bull.* **58** (1974) 2295; b) Orr, W.L., *Adv. Org. Geochem.* **1977**, 571; c) Anisimov, L.A., *Geochem. Internat.*, **15** (1978) 63; d) Aizenshtat, Z., 205th ACS National Meeting, Book of Abstracts, Div. Geochem. p. 76, Denver, 1993; e) Goldstein, T.P., and Aizenshtat, Z., *J. Therm. Anal.* **42** (1994) 241.
- [2] Pryor, W.A., Ed. "Mechanisms of Sulfur Reactions", McGraw-Hill, New York, (1962).
- [3] E.g.: Fromm, E., and Acker, O., *Ber. Dtsch. Chem. Ges.* **36** (1903) 538.
- [4] Steinfatt, I., and Hoffmann, G.G., *Phosphorus, Sulfur, and Silicon*, **74** (1993) 431.
- [5] Fedorak, P.M., in "Geochemistry of Sulfur in Fossil Fuels", Orr, W.L., and White, C.M., Eds., ACS Symposium Series 429, Washington, DC, p. 93 (1990).
- [6] Hoffmann, G.G., Steinfatt, I., David, T., and Strohschein, A., *DGMK Tagungsbericht 9501, Hamburg 1995*, p. 281.
- [7] Orr, W.L., and Sinnighe Damsté, J.S., in "Geochemistry of Sulfur in Fossil Fuels", Orr, W.L., and White, C.M., Eds., ACS Symposium Series 429, Washington, DC, p. 2 (1990).
- [8] E.g.: a) Siskin, M., Brons, G., Katritzky, A.R., and Balasubramanian, M., *Energy & Fuels* **4** (1990) 475; b) Siskin, M., Brons, G., Katritzky, A.R., and Murugan, R., *Energy & Fuels* **4** (1990) 482; c) Siskin, M., Glen, B., and Vaughn, S.N., *Energy & Fuels* **4** (1990) 488; d) Katritzky, A.R., Lapucha, A.R., Murugan, R., and Luxem, F.J., *Energy & Fuels* **4** (1990) 493; e) Katritzky, A.R., Balasubramanian, M., and Siskin, M., *Energy & Fuels* **4** (1990) 499; f) Katritzky, A.R., Lapucha, A.R., and Siskin, M., *Energy & Fuels* **4** (1990) 506; g) Katritzky, A.R., Lapucha, A.R., and Siskin, M., *Energy & Fuels* **4** (1990) 510; h) Katritzky, A.R., Luxem, F.J., and Siskin, M., *Energy & Fuels* **4** (1990) 514; i) Katritzky, A.R., Luxem, F.J., and Siskin, M., *Energy & Fuels* **4** (1990) 518; j) Katritzky, A.R., Luxem, F.J., and Siskin, M., *Energy & Fuels* **4** (1990) 525; k) Katritzky, A.R., Murugan, R., and Siskin, M., *Energy & Fuels* **4** (1990) 531; l) Katritzky, A.R., Murugan, R., and Siskin, M., *Energy & Fuels* **4** (1990) 538; m) Katritzky, A.R., Balasubramanian, M., and Siskin, M., *Energy & Fuels* **4** (1990) 543; n) Katritzky, A.R., Murugan, R., Balasubramanian, M., and Siskin, M., *Energy & Fuels* **4** (1990) 547; o) Katritzky, A.R., Lapucha, A.R., and Siskin, M., *Energy & Fuels* **4** (1990) 555; p) Katritzky, A.R., Lapucha, A.R., Greenhill, J.V., and Siskin, M., *Energy & Fuels* **4** (1990) 562; q) Katritzky, A.R., Lapucha, A.R., Luxem, F.J., Greenhill, J.V., and Siskin, M., *Energy & Fuels* **4** (1990) 572; r) Katritzky, A.R., Murugan, R., and Siskin, M., *Energy & Fuels* **4** (1990) 577; s) Katritzky, A.R., Allin, S.M., and Siskin, M., *Acc. Chem. Res.* **29** (1996) 399.
- [9] a) Oae, S., Ed. "Organic Chemistry of Sulfur", Plenum Press, New York, (1977) p. 360; b) Oae, S., and Togo, H., *Tetrahedron Lett.*, **23** (1982) 4701; c) Oae, S., and Togo, H., *Kagaku (Chemistry)* **38** (1983) 506; d) Oae, S., in "Review of Heteroatom Chemistry", Vol. 1, Oae, S., Ed., NYU, Tokyo, 1987, p. 14; e) Hoffmann, G.G. and Steinfatt, I., Preprints, Div. of Petrol. Chem., ACS, **38**, 1 (1993) 181; f) Hoffmann, G.G., Steinfatt, I., and Strohschein, A., in "Recent Advances in Oilfield Chemistry", Ogden, P.H., Ed., Special

Publication No. 159, Royal Society of Chemistry, Cambridge 1994, p. 189; g) Hoffmann, G.G., Steinfatt, I., and Strohschein, A., Proceedings SPE 29016, SPE International Symposium on Oilfield Chemistry, San Antonio, USA, Februar 1995, 745; h) Hoffmann, G.G., Steinfatt, I., and Strohschein, A., Proceedings, Vol. 1, 6<sup>th</sup>.UNITAR International Conference on Heavy Crude and Tar Sands, Houston, USA, Februar 1995, p.317.

- [10] a) Toland, W.G., US-Pat. 2722546, (Nov. 1, 1955) [Chem. Abstr. 57, 11111i (1955)]; b) Toland, W.G., J. Am. Chem. Soc., **82** (1960) 1911.  
 [11] Biswas, S.C., Sabhurwal, V.P., and Dutta, B.K., Fert. Tech. **13** (1976) 255; loc. cit.  
 [12] Schöninger, W., Mikrochim. Acta, **1956**, 869.  
 [13] Hoffmann, G.G., Steinfatt, I., and Bode, K., Erdöl, Erdgas Kohle, **2** (1996) 70.  
 [14] Wiley Database, HP 59943B; a merged Wiley/NBS database.

Table 1. Parameters of the Reactions

No.	sulfate [20 mmol]	organic compounds [5 ml]	pressure [bar]	temperature [°C]	time [h]	reduction [%]	pH-value (after the reaction)
1	(NH <sub>4</sub> ) <sub>2</sub> SO <sub>4</sub>	--	162	350	46	none	7.0
2	MgSO <sub>4</sub>	octane	--	320	72	none	7.0
3	CaSO <sub>4</sub>	toluol	--	290	288	none	5.0
4	Na <sub>2</sub> SO <sub>4</sub>	octane	126	320	72	3	7.5
5	Na <sub>2</sub> SO <sub>4</sub>	octane	145	320	500	11	7.5
6	MgSO <sub>4</sub>	octane	74	250	72	4	6.3
7	MgSO <sub>4</sub>	octane	90	270	72	6	6.1
8	MgSO <sub>4</sub>	octane	124	300	72	41	6.7
9	MgSO <sub>4</sub>	octane	156	320	72	66	6.8
10	MgSO <sub>4</sub>	octane	--	320	24	27	6.8
11	MgSO <sub>4</sub>	octane	--	320	48	37	6.8
12	MgSO <sub>4</sub>	octane	--	320	144	97	6.5
13	CaSO <sub>4</sub>	octane	39	200	72	none	2.9
14	CaSO <sub>4</sub>	octane	--	250	72	22	3.8
15	CaSO <sub>4</sub>	octane	--	270	72	46	3.6
16	CaSO <sub>4</sub>	octane	--	290	72	76	5.5
17	CaSO <sub>4</sub>	octane	178	320	72	83	6.2
18	CaSO <sub>4</sub>	octane	159	320	9	54	4.6
19	CaSO <sub>4</sub>	octane	--	320	36	77	6.1
20	CaSO <sub>4</sub>	octane	188	320	144	88	6.6
21	CaSO <sub>4</sub>	octane	174	320	288	89	7.3
22	Al <sub>2</sub> (SO <sub>4</sub> ) <sub>3</sub>	octane	23	100	72	10	3.4
23	Al <sub>2</sub> (SO <sub>4</sub> ) <sub>3</sub>	octane	44	200	72	96	3.5
24	Al <sub>2</sub> (SO <sub>4</sub> ) <sub>3</sub>	octane	160	320	72	99	4.1
25	Al <sub>2</sub> (SO <sub>4</sub> ) <sub>3</sub>	octane	--	320	6	98	3.6
26	MgSO <sub>4</sub>	hexadecane	--	320	72	83	6.4
27	MgSO <sub>4</sub>	2-octanone	--	320	72	79	6.6
28	MgSO <sub>4</sub>	crude oil*	101	290	72	34	7.1
29	CaSO <sub>4</sub>	crude oil*	--	270	72	31	--
30	CaSO <sub>4</sub>	crude oil*	--	320	72	83	6.0

\*: 30 g crude oil; 60 mmol of the corresponding sulfate

Table 2a. Analytical Data of GC

Injector temperature (°C)	280
FID temperature (°C)	330
FPD temperature (°C)	250
GC column	DB 5, 30 m x 0.25 mm, film thickness 0.25 µm
Carrier gas	Helium
Carrier gas flow (ml/min.)	1
Sample size (µl)	1
Split	1:35
Initial oven temp. (°C)	35
Initial hold (min.)	5
Program rate (°C/min.)	5
Final oven temp. (°C)	310
Final hold (min.)	10

Table 2b. Analytical Data of GC/MS

Initial Injector temp. (°C)	40
Program rate (°C/s)	12
Final Injector temp. (°C)	300
Final hold (min.)	10
Purge time (min.)	5
GC/MS column	DB 1, 30 m x 0.25 mm, film thickness 0.25 µm
Carrier gas	Helium
Carrier gas flow (ml/min.)	1
Sample size (µl)	0.15
Initial oven temp. (°C)	35
Initial hold (min.)	5
Program rate (°C/min.)	5
Final oven temp. (°C)	310
Final hold (min.)	10

Table 3. Products of Reactions at 320°C for 72 hrs. (Tab.1: 9, 26, 27)

Products from <i>n</i> -octane	Products from <i>n</i> -hexadecane	Products from 2-octanone
1. 2-Methyltetrahydro-t.	1. 2-Methylthiophene	1. Heptane
2. Ethylbenzene	2. 2-Methyltetrahydro-t.	2. 2-Methylthiophene
3. 2-Ethylthiophene	3. 2-Ethylthiophene	3. 1-Ethyl-2-methyl-cyclopentane
4. 2,5-Dimethylthiophene	4. 2,5-Dimethylthiophene	4. Octene
5. <i>o</i> -Xylene	5. 2-Propylthiophene	5. Ethylbenzene
6. 2-Propylthiophene	6. 2-Ethyl-5-methyl-t.	6. 2-Ethylthiophene
7. 2-Ethyl-5-methyl-t.	7. 2-Methyl-propyl-t.	7. 2,5-Dimethylthiophene
8. 4-Octanone	8. Benzo[b]thiophene	8. <i>o</i> -Xylene
9. 3-Octanone	9. 3-Hexadecanone	9. 1-Ethyl-5-Methyl-t.
10. 2-Octanone	10. 2-Heptyl-5-pentyl-t.	10. 2,5-Diethylthiophene
11. 2-Methyl-5-propyl-t.	11. 2-Butyl-5-octyl-t.	11. 2-Methyl-5-propyl-t.
12. 2-Butylthiophene	12. 2-Nonyl-5-propyl-t.	12. 2-Butyltetrahydro-t.
13. 2,2-Bithiophene	13. 2-Decyl-5-ethyl-t.	13. Benzo[b]thiophen
	14. 2-Methyl-5-undecyl-t.	
	15. 2-Dodecylthiophene	

t.: abbreviation for thiophene

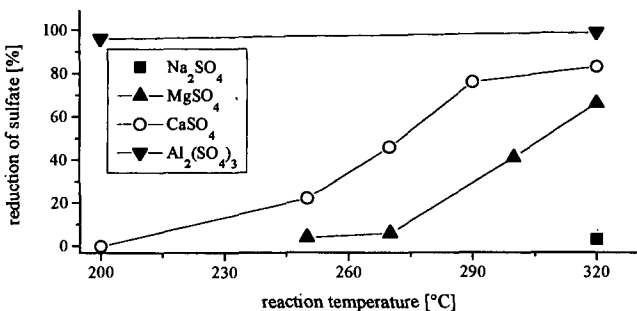


Figure 1. Influence of Temperature and Cation on the Reduction of Sulfate (t = 72 hrs.)

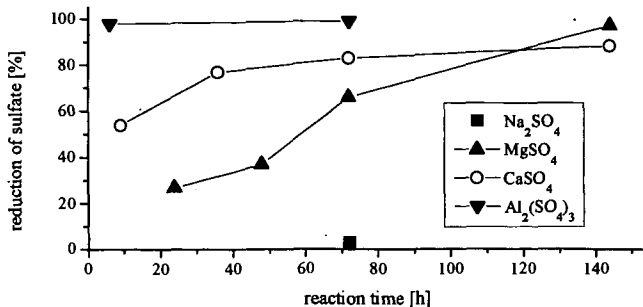


Figure 2. Influence of Reaction Time and Cation on the Reduction of Sulfate (T = 320°C)

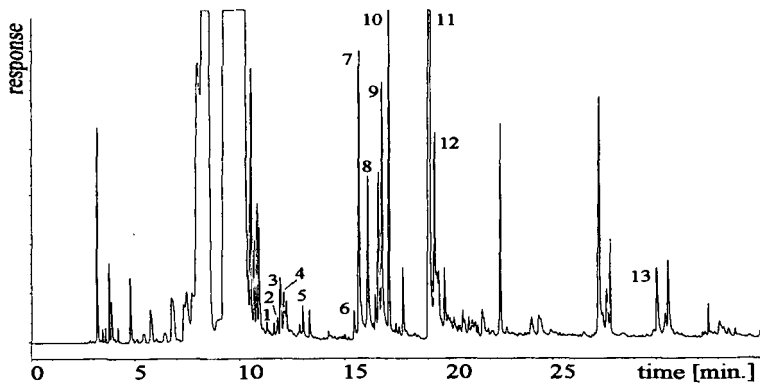


Figure 3. FID Chromatogram of the Reaction of  $\text{MgSO}_4/\text{H}_2\text{S}/\text{Octane}$  at  $320^\circ\text{C}$  (Tab.1: 9)

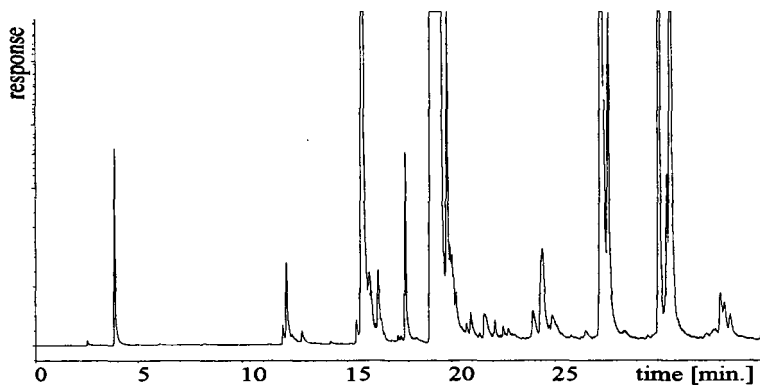


Figure 4. FPD Chromatogram of the Reaction of  $\text{MgSO}_4/\text{H}_2\text{S}/\text{Octane}$  at  $320^\circ\text{C}$  (Tab.1: 9)

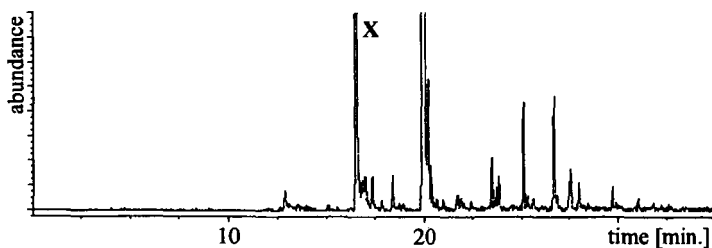


Figure 5. Ion Chromatogram of Ion 111.00 amu.

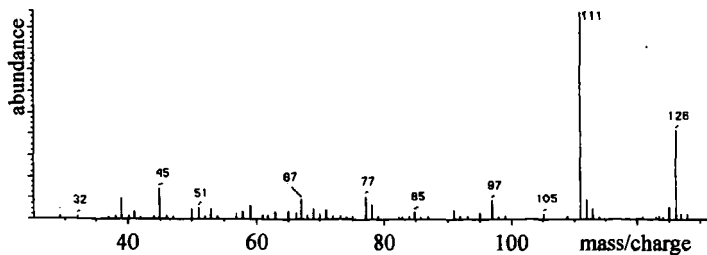


Figure 6. One (Peak Maximum) Scan of Compound X in Fig. 5

# HYDROGEN FROM BIOMASS VIA FAST PYROLYSIS AND CATALYTIC STEAM REFORMING

D. Wang, S. Czernik, D. Montané<sup>1</sup>, M. Mann, and E. Chomet<sup>2</sup>  
National Renewable Energy Laboratory (NREL)  
Golden, CO 80401-3303

Keywords: Hydrogen production, biomass, catalytic steam reforming

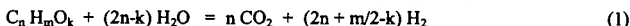
## ABSTRACT

Fast pyrolysis transforms biomass into "bio-oil", with yields as high as 75-80 wt.% of the anhydrous biomass. This bio-oil is a mixture of aldehydes, alcohols, acids, oligomers from the constitutive carbohydrates and lignin, and some water from the dehydration reactions. Tests performed using a microreactor interfaced with a molecular beam mass spectrometer and a bench-scale, fixed bed reactor have demonstrated near stoichiometric hydrogen yields from steam reforming of the bio-oil aqueous fraction obtained after precipitation and separation of the lignin-derived oxyaromatics. Reforming of the aqueous fraction required proper dispersion of the liquid to avoid vapor-phase carbonization of the feed in the inlet to the reactor. A spraying nozzle injector has been designed and successfully tested. We will present and discuss the process developed for the pyrolysis and reforming operations and some preliminary product cost estimates. The economics of the process is favored when the separated lignin-derived oxyaromatics are converted to valuable co-products and the aqueous fraction of the bio-oil is used for hydrogen production.

## INTRODUCTION

Although renewable lignocellulosic biomass has been considered as a potential feedstock for gasification to produce syngas, the economics of current processes favor the use of hydrocarbons (natural gas, C<sub>2</sub>-C<sub>5</sub>, and naphtha) and inexpensive coal. An alternative approach to the production of H<sub>2</sub> from biomass is fast pyrolysis of biomass to generate a liquid product (also known as bio-oil) and catalytic steam reforming of the oil or its fractions. This latter approach has the potential to be cost competitive with the current commercial processes for hydrogen production. The yield of bio-oil can be as high as 75-80 wt.% of the anhydrous biomass.

Bio-oil is a mixture of aldehydes, alcohols, acids, oligomers from the constitutive carbohydrates and lignin, and some water from the dehydration reactions. The overall steam reforming reaction of bio-oil (or any oxygenate with a chemical formula of C<sub>n</sub>H<sub>m</sub>O<sub>k</sub>), is given by:



The stoichiometric yield of hydrogen is  $2+m/2n-k/n$  moles per mole of carbon in the feed, and  $k/n$  is usually in the fractions for the aromatic phenolics from lignin, while  $k/n$  is close to 1 for most carbohydrate-derived products such as sugars. In contrast to producer gas, *bio-oil* is easily transportable. Thus, the two key process steps, pyrolysis and reforming, can be carried out independently at different locations. This allows to minimize the costs of feedstock, transportation, and product (H<sub>2</sub>) distribution. In this paper, we describe results on catalytic steam reforming of oxygenates. Tests performed using a microreactor interfaced with a molecular beam mass spectrometer and a bench-scale, fixed bed reactor have demonstrated near stoichiometric hydrogen yields from the bio-oil aqueous fraction obtained after precipitation and separation of the lignin-derived oxyaromatics. We will also present results of preliminary economic analysis on this process, which also produces a valuable co-product (lignin-derived oxyaromatics).

## EXPERIMENTAL

Tests were carried out in two systems: a microreactor coupled to a molecular-beam mass spectrometer (MBMS) and a bench-scale fixed bed unit. Both systems have been described in detail in our previous work.<sup>1,2</sup> The microreactor was housed in a tubular furnace with four independently controlled temperature zones. The dual bed configuration of this reactor enabled us to study either the differences between thermolysis and catalysis or to compare the performances of two catalysts under the same temperature conditions. Gaseous products at the exit of the microreactor are sampled in real-time through a supersonic, free-jet expansion nozzle.

<sup>1</sup> On leave from Universitat Rovira i Virgili, Departament d'Enginyeria Química, Autovia de Salou S/N, Tarragona, 43006 Spain.

<sup>2</sup> Also affiliated with Université de Sherbrooke, Sherbrooke, Quebec, Canada, J1K-2R1

This expansion cools the reaction products and forms a molecular beam that is ionized and analyzed by a quadrupole mass spectrometer.

The bench-scale reactor is a stainless steel tube (1.65 cm id x 42.6 cm length) housed in a tubular furnace equipped with three independently controlled heating zones. The reactor was packed with about 100 g of a commercial, nickel-based catalyst (particle size: 2.4-4.0 mm). Most studies were carried out using the UCI G-90C catalyst and a dual-catalyst bed of 46-1 and 46-4 from ICI Katalco. Steam was generated in a boiler and superheated. The organic feed from a diaphragm metering pump was sprayed using N<sub>2</sub> and mixed with superheated steam in a triple nozzle injector. Products exiting the reactor were passed through a condenser. The condensate (just water in most cases) weight, volume and compositions of the permanent gas output were recorded periodically. An on-line IR gas analyzer was used to monitor CO/CO<sub>2</sub> concentrations and a MTI-QUAD GC was used to measure concentrations of H<sub>2</sub>, N<sub>2</sub>, O<sub>2</sub>, CO, CO<sub>2</sub>, CH<sub>4</sub>, and other light hydrocarbons. The reformer system was interfaced with a computer to monitor temperatures and other important parameters. All materials used were obtained from commercial suppliers, except the bio-oil and its aqueous fraction that were prepared at NREL.

## RESULTS AND DISCUSSION

**Rapid Screening Studies.** The goal of these experiments was to demonstrate the high efficiency of catalytic steam reforming as a method for conversion of bio-oil to hydrogen, with specific objectives to evaluate and select best catalysts and operating conditions, and to gain mechanistic insight into the chemistry involved in the steam reforming reactions of oxygenates. A series of model oxygen-containing compounds, biomass and its main components (cellulose, xylan, and lignin), and *bio-oil* and its various fractions were screened under identical conditions using a commercial catalyst, G-90C, from United Catalyst Inc. (UCI). We also tested a number of research and commercial steam reforming catalysts and a WGS catalyst and determined H<sub>2</sub> yields using four model compounds (methanol, acetic acid, an aqueous solution of hydroxyacetaldehyde, and a methanol solution of 4-allyl-2,6-dimethoxyphenol) under the same operating conditions. All of the catalysts tested were capable of reforming the model compounds and high conversions (>99%) were observed. The H<sub>2</sub> yields for all catalysts and model compounds were high, averaging 90% (±5%) of the stoichiometric. Within our experimental error limit, there is no clear indication of one catalyst being better than the others. Among the most important parameters for steam reforming are catalyst bed temperature (T), molar steam-to-carbon ratio (S/C), gas hourly space velocity (G<sub>C1</sub>HSV), and residence time (t, calculated from the void volume of the catalyst bed divided by the total flow rate of gases at the inlet of the reactor; void fraction = 0.4). Temperature was found to have the most profound effect on steam reforming reactions. Within experimental error limits, varying residence time from 0.04 to 0.15 s and increasing S/C from 4.5 to 7.5 showed no significant effects on the yield of hydrogen under the conditions of 600°C and GHSV (gas hourly space velocity, on C<sub>1</sub> basis) = 1680 h<sup>-1</sup>; however, this affected the yield of CH<sub>4</sub>.

From these rapid screening studies of various classes of model oxygenate compounds, we found that steam reforming of oxygenates generally involves a significant competition from the decomposition owing to thermally-induced cracking prior to entering the catalyst bed and the acid-catalyzed reactions at the acidic sites of the catalyst support. These competing thermal decomposition reactions may result in the formation of carbonaceous materials (coke), blocking the reactor and even deactivating the catalyst. This calls for special emphasis on how to feed bio-oil or its fractions into the reactor. However, a complete conversion of both the oxygenate feed and its decomposition products to hydrogen can be achieved with commercial Ni-based catalysts under reasonable operating conditions, if char formation prior to reaching the catalyst bed and coking on the catalyst can be eliminated, or at least controlled.

**Bench-Scale Tests.** Tests at the bench-scale level were conducted to obtain the global and elemental mass balances and the carbon-to-gas conversion, to quantify the distribution of gas products under conditions of complete conversion of the pyrolysis oil feedstock, and to study catalyst lifetime and regeneration. We used both model compounds (methanol, acetic acid, syringol and *m*-cresol, both separately and in mixtures) and real bio-oil (its aqueous fraction), and representative results are listed in Table 1. Profiles of the output gas composition are shown for the 3-component mixture in Figure 1 and for the poplar oil aqueous fraction in Figure 2. The following discussions are focused on the reforming of a 3-component mixture and a bio-oil aqueous fraction.

The three-component mixture contained 67% acetic acid, 16% *m*-cresol, and 16% syringol. Its composition was close to the proportions of the carbohydrate fraction and the lignin fraction in bio-oil. We observed *some coke deposits* on the top portion of the UCI G-90C catalyst bed. The overall mass balance (carbon, hydrogen, and oxygen) was 99% and the carbon conversion to gas was 96% (Table 1). The other catalyst tested for steam reforming of the 3-component mixture was the 46-series from ICI Katalco (46-1/46-4). This dual catalyst bed is used in commercial naphtha reforming plants to reduce coke formation and extend catalyst lifetime. It showed an excellent and steady performance *without any coke deposition* on the catalyst. The gas composition (Figure 1) remained constant throughout the whole run. The overall mass balance (including carbon, hydrogen, and oxygen) was 104%, and for carbon 105%, indicating that there may be a systematic error in our measurement. An excellent hydrogen yield of 86% was obtained, and the total hydrogen potential may be as high as 98% with a second water-gas shift reactor. These results confirm that both the UCI G-90C and especially the ICI 46-series catalysts can efficiently convert oxygenates to hydrogen.

Steam reforming of bio-oil or its fractions was found to be more difficult than that of model compounds. The main problem that needed to be solved was feeding the oil to the reactor. Bio-oil cannot be totally vaporized; significant amounts of residual solids are often formed that block the feeding line and the reactor. Thus, the simple injection system used for model compounds had to be modified to allow spraying bio-oil and its fractions in to the catalytic reactor without prior char formation.

A poplar oil generated in the NREL vortex reactor system was extracted using ethyl acetate (EA) and water (weight ratios of 1:1:1 for oil:EA:water). The resulting aqueous fraction (55% of the whole oil) contained 25% organics and 75% water. It was successfully fed to the reactor using a triple-nozzle spraying system with minimal accumulation of char in the reactor inlet. A large excess of steam (S/C = 20-30) was used, together with a high flow rate of nitrogen, to allow for proper oil dispersion and heat transfer required to maintain a sufficiently high temperature (>500°C) at the reactor entrance. A portion of water and other volatiles in the sprayed droplets evaporate during mixing with the superheated steam and the remaining will contact the catalyst surface directly. The ICI 46-series catalysts performed satisfactorily with no coke formation. We observed a stable gas production rate and composition throughout the whole 4-hour-long experiment (Figure 2).

The carbon conversion of the aqueous fraction to gas products was almost quantitative in both runs that used the same catalyst bed (Table 1). We observed similar levels of mass balances as in the experiments using model compounds: global 99%, carbon 105%, and hydrogen 97%. The methane concentration (with N<sub>2</sub> excluded) increased from 0.56% in the first run (2 h, t=0.03 s) to 2.2% in the second run (4 h, t=0.02 s), and both values were much higher than that (0.01%) obtained from the 3-component model compound mixture (17 h, t=0.09 s). This was likely caused by the shorter residence time forced by the large flow rate of steam and nitrogen used in the experiment.

*Process Design and Preliminary Economics.* In the process being evaluated, bio-oil generated from fluid bed pyrolysis of biomass will be refined through a separation step (using water and ethyl acetate) to recover an oxyaromatic coproduct which will be used as a phenolic substitute in resin formulations. The remaining aqueous fraction will be catalytically steam reformed to produce hydrogen, using a process based on that used for natural gas reforming. Because of the low sulfur content of biomass and bio-oil, a sulfur removal system is not likely to be required. Also, according to thermodynamic simulations and the screening results, a temperature reformer ramping up to 700°-750°C (which is lower than 825°-900°C required for reforming natural gas) will be needed. The ratio of steam to oil will be determined by experimental results and economic optimization; it will be in the 5 to 7 range, based on the literature and experimental data already obtained. Laboratory experiments will provide the basis for the choice of the most suitable catalyst and reactor configuration; the base case will use a fixed-bed catalytic reactor. A pressure swing adsorption unit will be used to purify the H<sub>2</sub> produced.

A feasibility analysis was performed on this process to determine if the process could have economic viability and specify areas where research will help to lower the production cost.<sup>3</sup> Both laboratory data and standard process data, where applicable, were used. Although this analysis is not of design quality, it does provide useful information on this research project before scale-up and commercialization. The capital investment of the pyrolysis plant was taken from Beckman and Graham.<sup>4</sup> Biomass was considered available at a cost of \$25/dry tonne. A

15% internal rate of return was assumed for both the pyrolysis and reforming facilities. The phenolics substitute coproduct was assumed to be sold for \$0.44/kg, a fraction of the selling price of phenol. Steam is produced through heat integration and is sold as a by-product.

For our conceptual process, the cost of hydrogen has been estimated to be \$7.70/GJ for the base case (production capacity: 35.5 tonne of hydrogen per day), falling within the range of the current selling price of  $H_2$  in industry (\$5-14/GJ). Several parameters (for instance, a lower cost for biomass) can lower this price to \$3-5/GJ.<sup>3</sup> The process can also sustain large changes in coproduct selling price, capital cost, and hydrogen production capacity before the hydrogen becomes more expensive than current markets will allow.

## CONCLUSIONS

Reforming biomass-derived oxygenates appears to be possible using available Ni-based catalysts. It involves both thermal decomposition of the labile oxygenates and the catalytic steam reforming of the starting material and its decomposition products. At least 80% of the theoretical maximum hydrogen yield has already been obtained. The excess steam can be reduced to achieve S/C on the order of 5-10, as in cases of natural gas and naphtha reforming, by modification of reactor design. Fast pyrolysis followed by reforming represents a credible alternative to gasification with the following advantages: no oxygen is needed; a co-product strategy is possible; a regionalized system of production units coupled to a central reformer offers greater flexibility. Low biomass costs are required to produce hydrogen economically since feedstock cost is a significant component of the production cost. Co-products from the pyrolysis oil favor the economics.

## REFERENCES

1. Wang, D.; Montané, D.; Chornet, E. *Applied Catalysis A: General* **1996**, *143*, 245-270.
2. Chornet, E.; Wang, D.; Czernik, S.; Montané, D.; Mann, M. In *Proceedings of the 1996 U.S. DOE Hydrogen Program Review*. NREL/CP-430-21968, May 1-2, 1996, Miami, Florida. pp 457-480.
3. Mann, M.; Spath, P.; Kadam, K. In *Proceedings of the 1996 U.S. DOE Hydrogen Program Review*. NREL/CP-430-21968, May 1-2, 1996, Miami, Florida. pp 249-272.
4. Beckman, D. and Graham, R. In *Advances in Thermochemical Biomass Conversion*, (ed. A.V. Bridgwater) Blackie Academic & Professional, London, 1993. pp. 1314-24.

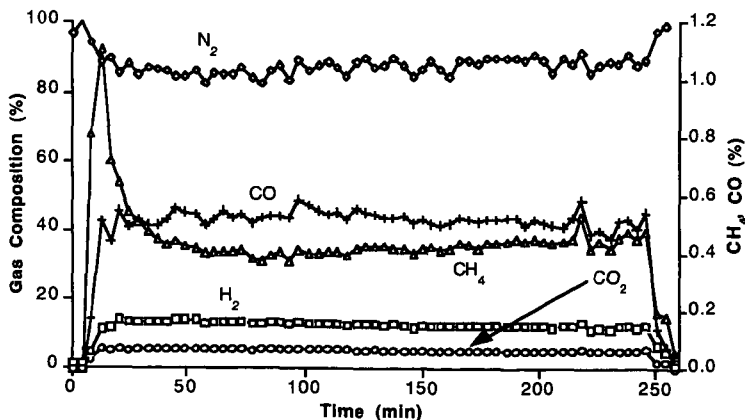


Figure 2. Composition of gaseous products during the steam reforming of a bio-oil aqueous fraction using the ICI 46-series catalyst.

Table 1. Summary of results for catalytic steam reforming experiments on the bench-scale reformer

Feed	Catalyst	S/C <sup>a</sup>	GC <sub>1</sub> HSV <sup>b</sup>	Temperatures (°C)			Yield (mol/100 mol of carbon fed)				% Carbon-gas conversion	% st. yield of H <sub>2</sub> (+WGS) <sup>c</sup>	Time on stream (h)
				Top	Middle	Bottom	H <sub>2</sub>	CO <sub>2</sub>	CO	CH <sub>4</sub>			
acetic acid	UCI G-90C	4.7	1973	685	716	833	145.8	50.3	49.7	0.055	101	73 (98)	6
acetic acid	UCI G-90C	12.8	777	710	789	830	171.8	74.9	29.0	0.005	104	86 (100)	8
syringol (in MeOH)	UCI G-90C	6.3	2454	702	745	830	195.0	45.4	53.9	0.2	100	75 (96)	4
syringol (in MeOH)	UCI G-90C	7.4	1985	750	803	863	197.3	46.0	54.9	0.1	101	76 (97)	4
3-component mixture	UCI G-90C	6.5	1053	738	NA	833	167.6	67.4	28.6	0.00	96	78 (91)	11
3-component mixture	ICI 46-1/46-4	4.9	1053	782	753	834	187.8	79.8	27.4	0.03	105	86 (98)	17
poplar oil aq. fraction	ICI 46-1/46-4	19.3	1110	480	730	818	206.7	85.2	9.6	1.7	97	103 (108)	2
poplar oil aq. fraction	ICI 46-1/46-4	30.0	1000	530	744	821	205.8	86.6	8.4	6.9	102	103 (107)	4

<sup>a</sup> Molar ratio of steam to carbon. <sup>b</sup> Gas hourly space velocity on C<sub>1</sub> basis (h<sup>-1</sup>). <sup>c</sup> Assuming all CO being converted to H<sub>2</sub> in a down stream WGS unit. NA = not available.

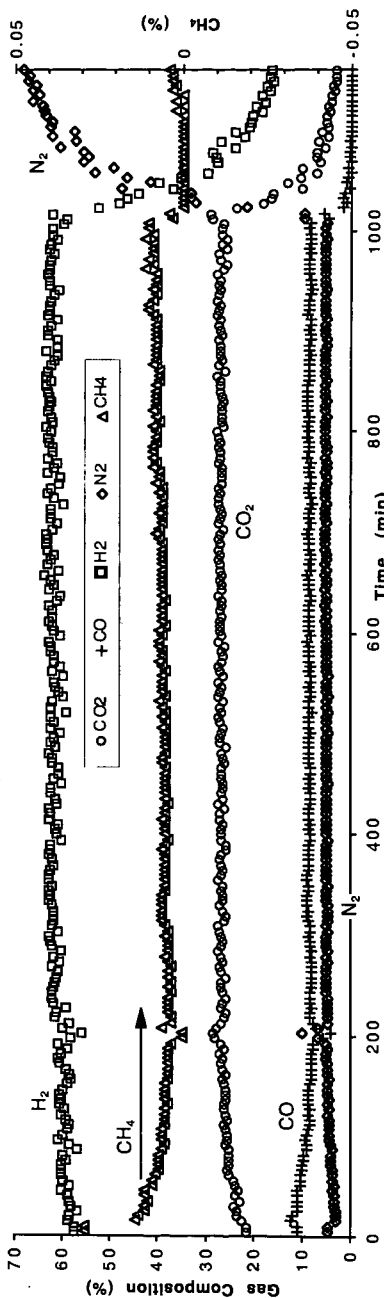


Figure 1. Composition of gaseous products during steam reforming of a 3-component mixture using the ICI 46-series catalyst.